J. Appl. Comput. Mech., 9(3) (2023) 775-803
DOI: 10.22055/jacm.2023.41985.3851

ISSN: 2383-4536
jacm.scu.ac.ir

Shahid Chamran University of Ahvaz

Journal of Applied and Computational Mechanics

Review Paper

Smart Gas Sensors: Materials, Technologies, Practical Applications, and Use of Machine Learning – A Review

Lubna Mahmood[1], Mehdi Ghommem[2], Zied Bahroun[3]

[1] Engineering Systems Management Graduate Program, American University of Sharjah, Sharjah, P.O. Box 26666, United Arab Emirates, Email: lubnasmahmood@gmail.com
[2] Department of Mechanical Engineering, American University of Sharjah, Sharjah, P.O. Box 26666, United Arab Emirates, Email: mghommem@aus.edu
[3] Department of Industrial Engineering, American University of Sharjah, Sharjah, P.O. Box 26666, United Arab Emirates, Email: zbahroun@aus.edu

Received September 26 2022; Revised December 13 2022; Accepted for publication January 10 2023.
Corresponding author: M. Ghommem (mghommem@aus.edu)

Abstract. The electronic nose, popularly known as the E-nose, that combines gas sensor arrays (GSAs) with machine learning has gained a strong foothold in gas sensing technology. The E-nose designed to mimic the human olfactory system, is used for the detection and identification of various volatile compounds. The GSAs develop a unique signal fingerprint for each volatile compound to enable pattern recognition using machine learning algorithms. The inexpensive, portable and non-invasive characteristics of the E-nose system have rendered it indispensable within the gas-sensing arena. As a result, E-noses have been widely employed in several applications in the areas of the food industry, health management, disease diagnosis, water and air quality control, and toxic gas leakage detection. This paper reviews the various sensor fabrication technologies of GSAs and highlights the main operational framework of the E-nose system. The paper details vital signal pre-processing techniques of feature extraction, feature selection, in addition to machine learning algorithms such as SVM, kNN, ANN, and Random Forests for determining the type of gas and estimating its concentration in a competitive environment. The paper further explores the potential applications of E-noses for diagnosing diseases, monitoring air quality, assessing the quality of food samples and estimating concentrations of volatile organic compounds (VOCs) in air and in food samples. The review concludes with some challenges faced by E-nose, alternative ways to tackle them and proposes some recommendations as potential future work for further development and design enhancement of E-noses.

Keywords: Gas sensor arrays; E-nose; Disease diagnosis; Leakage detection; Machine learning; Volatile organic compounds.

1. Introduction

Over the last few years, gas sensing technology has garnered immense popularity for its wide-range applications in several industries. Gas sensors help in identifying and detecting various chemical compounds and are used for several applications. These include:

- Quality control in the food industry such as evaluating the freshness of meat [1] and detecting toxins in packaged food [2].
- Air quality control such as detecting radon concentration [3] and indoor air quality monitoring [4, 5].
- Disease diagnosis such as liver disease detection [6] and Alzheimer's detection [7].
- Gas leakage detection [8, 9].
- Hazard detection such as in livestock environment [10].

These sensors typically operate to generate an outcome usually in the form of an electrical signal that provides relevant information about the target gas. Owing to their contribution in numerous industries, gas sensors are required to be small and cost-effective so that they can be easily integrated with other systems. This allows them to properly identify and detect target gases as per the application of interest. The performance of gas sensors is usually assessed by four crucial metrics: selectivity, sensitivity, stability, and response time [11, 12]. Selectivity is defined as the ability of the gas sensor to detect a specific gas in a competitive environment characterized by the presence of a variety of gases. Sensitivity is defined as the change in the sensor output per unit change of the input [13]. Under normal conditions, as opposed to tightly controlled operation conditions, the gas sensors can be exposed to and affected by several gases of varying concentrations [14]. In such circumstances, the reliability of the gas sensors is driven by their ability to be extremely selective towards the gas of particular interest, and in several applications, be sensitive towards smaller concentrations of the gas. On the other hand, stability refers to the sensors' capacity to reproduce the sensor response over a certain period of time, whereas, response time refers to the time taken by the sensor to render a meaningful sensory signal response [11]. The response time is a critical parameter, especially when dealing with toxic gases, as the detection needs to occur immediately to activate safety functionalities and avoid catastrophic consequences.

Gas sensors offer different functionalities and varying responses for different applications. As such, in many cases, the use of a single sensor may not be sufficient to satisfy the needs of the application. Some of the most crucial challenges faced by gas sensors include:

Published online: January 25 2023

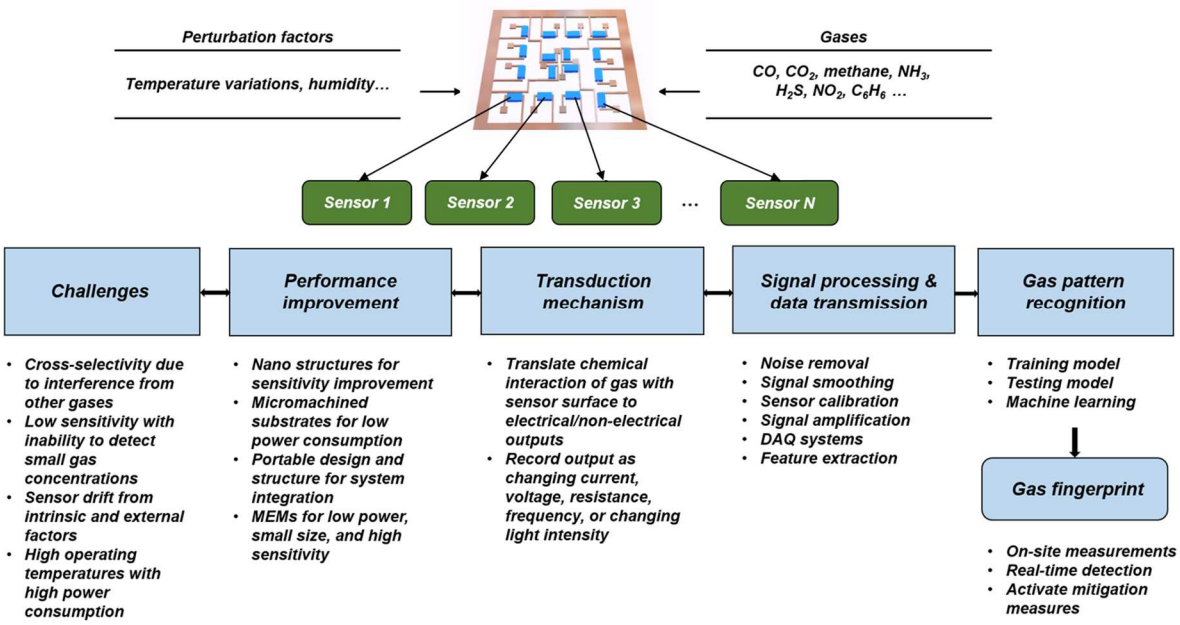

Fig. 1. Overall operation of the E-nose system using a GSA.

1) *Cross selectivity*: When detecting a certain target gas, the gas sensor might be exposed to other gases that may have similar properties as the target gas and this would interfere in the gas sensing [13, 14].

2) *Low sensitivity*: The operation of the gas sensor is highly impacted by the temperature and humidity of the surrounding environment [14–16]. Fluctuating temperature and humidity conditions could affect the ability of the gas sensor to detect the target gas, thereby, resulting in poor sensitivity that hinders the output of the desired sensory signal [17].

3) *Drift*: This is deemed as one of the most adverse challenges faced by gas sensors [18]. It is of two types: first-order drift, and second-order drift. First order drift occurs due to the interaction between the gas and the surface of the gas sensor, resulting in aging and poisoning of the gas sensor [19, 20] whereas second-order drift takes place due to external operating conditions, such as noise, temperature and humidity variations [21, 22].

Thus, to overcome these challenges, further developments in the gas sensing technology have led to the inception of the gas sensor array (GSA) that serves as a combination of different gas sensors with "processing capabilities" [11] and mimics the human olfactory system in detecting/identifying various chemical compounds. We show in Fig. 1 the different elements that contribute to the operation of the E-nose. The advent of GSAs has transpired the E-nose system that entails smart gas sensing technology based on machine learning. The E-nose combines GSAs with machine learning to detect the presence and identify chemical compounds, with improved accuracy and precision [11, 14]. Moreover, GSAs that combine gas sensors from different technologies are capable of detecting the target gases while improving selectivity and minimizing drift. In the E-nose applications, the prediction of the nature of the target gas (*classification*) and the estimation of its concentration (*regression*) is achieved through machine learning algorithms that fall under the umbrella of supervised learning. Machine learning techniques of feature extraction and feature selection enable to capture the most relevant characteristics of the target gas from the signal response. These characteristics, commonly referred to as *features*, are further processed by machine learning models to perform classification and regression tasks. However, owing to the adversities rendered by drift, GSAs result in different responses to the same target gas over long periods of time [13, 14, 21]. This has severely impacted the performance of machine learning algorithms while augmenting the maintenance costs associated with E-noses [21]. To combat these predicaments, researchers have attempted to propose several solutions that can help to improve the reliability of E-noses by ameliorating the predictive capability of the machine learning algorithms.

The present review highlights research studies conducted in gas sensing technology and the use of machine learning techniques to support this technology. It is organized as follows: Section 2 discusses different gas sensing materials; Section 3 provides a detailed discussion of machine learning techniques for feature extraction and feature selection, and machine learning models; Section 4 reviews the applications of E-nose in health management, food quality control and environmental management; and Section 5 presents some challenges associated with the deployment of E-nose systems and proposes some recommendations as potential future work.

2. Gas Sensing Materials and Technology

Gas sensors are manufactured using different materials based on the requirements of the application and each type of gas sensor detects the presence of the chemical compound to produce a unique sensor response. Feng et al. [14] demarcated the different types of sensors into two different categories based on their working principle as shown in Fig. 2. Gas sensing materials that operate based on electrochemical properties include the metal oxide (MoX) semiconductor, conductive polymer composite (CPC) and carbon nano-materials. On the other hand, the acoustic, optical, catalytic and metal organic framework (MOF)-based sensors rely on other properties for gas detection as will be discussed in the following sections.

2.1 Metal oxide semiconductor-based gas sensors

Amongst the gas sensing materials, metal oxide (MoX) semiconductor-based technology comprises the most widely used gas sensors. The most commonly used manufacturing materials are ZnO [42], SnO_2, Fe_2O_3, Ga_2O_3 and CuO [43, 44]. The sensing mechanism of MoX-based sensors relies on the interaction of the oxygen molecules with the surface of the metal oxide sensing material and the target gas [45]. In the absence of the target gas and in the vicinity of the sensor as shown in Fig. 3 [46], the oxygen molecules are adsorbed onto the surface of the MoX sensor surface, which is usually fabricated using SnO_2. For an n-type semiconductor, this adsorption traps the electrons which are then freed when the sensor is exposed to the reducing target gas.

Table 1. Types of gas sensors and their characteristics.

Sensor Type	Working Mechanism	Output Response	Characteristics	Reference
MoX	Interaction of oxygen molecules with metal oxide material	Change in sensor resistance	Portable Inexpensive Low selectivity/sensitivity	[23–26]
Conductive Polymer	Charge acquisition through interaction with target gas	Change in sensor resistance	Good sensitivity Expensive	[27, 28]
Carbon-nanotube	Adsorption of target gas on the walls of nanotubes	Change in sensor resistance	High sensitivity Fast response time	[29, 30]
Acoustic	Adsorption of the gas on the vibrating material	Change in oscillating frequency	High sensitivity Expensive	[31, 32]
Catalytic	Oxidation of the target gas on the surface of the sensor	Change in heat released	Inexpensive Low selectivity/sensitivity	[33, 34]
Metal Organic Framework (MOF)	Vibration through 1st and 2nd order modes for multi-stimuli detection	Change in vibration amplitude, shift in vibration frequency	High sensitivity Low power consumption Portable	[35-37]
Optical sensors	Interaction of the gas molecules with radiation from light source	Change in intensity of the emitted radiation	Portable High sensitivity Fast response time	[38-41]

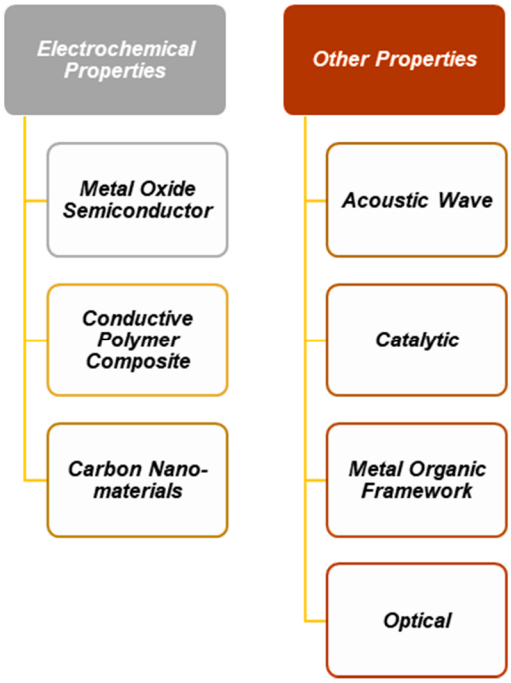

Fig. 2. Different types of sensors used in gas sensing.

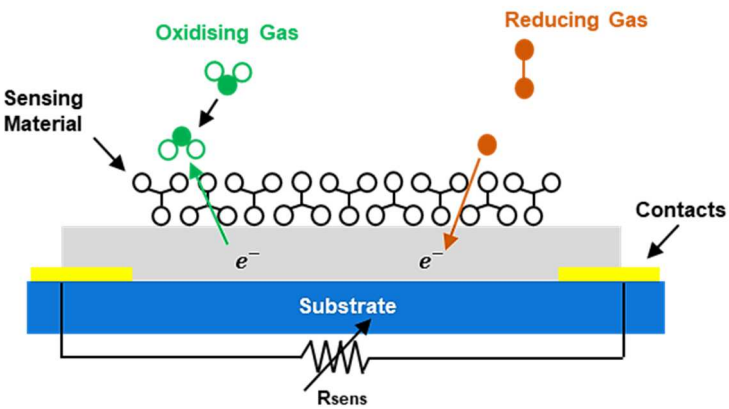

Fig. 3. Working of a typical MoX sensor for gas detection [46] © (2017) IEEE.

Once exposed to the reducing gas, the oxygen is desorbed from the surface of the sensing material, resulting in the flow of current (See Fig. 3) and thereby, increasing the electrical conductivity of the surface material. In case of an oxidizing target gas exposed to a p-type semiconductor, an increase in the concentration of electrons at the sensor surface results in the generation of holes, hence, decreasing the sensor electrical resistance (increasing conductivity). This electrical conductivity is measured in the form of a resistance change across the MoX surface [11], wherein the change in the resistance is directly proportional to the concentration of the target gas.

Table 1 summarizes the different types of gas sensors, their working mechanisms, and their characteristics. Depending on their operating principle, the output of the sensor can take different forms ranging from electrical resistance to frequency shift.

In addition, controlling the operating temperature helps in improving the affinity of the MoX-based sensor surface towards certain target gases [47]. Although these gas sensors are usually inexpensive, portable, and characterized by low power consumption, MoX-based sensors suffer from low selectivity and slow response time [11, 48]. Oosthuizen et al. [5] discussed the use of CuO nano-platelets to improve the selectivity and sensitivity of the sensor towards carbon monoxide (CO), whereas Rebholz and Grossmann [49] proposed selectivity enhancement of MoX sensors by fabricating double-layer MoX sensors using flame spray pyrolysis. Using a micromachined silicon-based hotplate gas sensor that yields low power consumption, Bierer et al. [50] attempted to measure the changing conductivity of the MoX sensor on exposure to a target gas. Besides measuring conductivity, the hotplate was capable of accounting for the change in the power consumption due to changing gases, thereby, improving the selectivity of the MoX gas sensor.

Moreover, researchers have attempted to counter the slow response time of these sensors using a double first-order model of the MoX-based sensor with acceptable results [47]. Addressing their low sensitivity, MoX sensors designed with micro and nano-sized film structures have shown great potential over the last few years [51]. The sensors designed with these structures produced a high surface-to-volume ratio rendering high sensitivity, which was further corroborated by testing gases like O_2, CO and NO_2. This is demonstrated by Faglia et al. [52], where they studied the performance of micromachined silicon substrates. Micromachined silicon substrates have been in use for several years and utilize semiconductor oxide layers for their operation [52, 53]. Faglia et al. [52] observed the impact of depositing a semiconductor oxide (Au doped SnO2) layer onto the substrate which helped to achieve low power consumption and higher sensitivity when detecting the target gas. Besides silicon substrates, research to find alternative substrate materials has paved the way for glass substrates [54], which were introduced to combat the fragility and the complex fabrication of silicon substrates.

2.2 Conductive polymer-based gas sensors

The conductive polymer composite (CPC) gas sensors are made up of non-conducting polymers and conductive filler materials such as carbon, graphite fibers that are dispersed in a polymer matrix [55], where the polymers and conductive fillers form the cornerstone for their sensing performance [56]. The materials used in the fabrication of these sensors are found to be gas-sensitive and operate well at room and low temperatures [14]. Owing to these properties of the conductive polymers, the CPCs are used to develop organic conducting polymers, known as intrinsically conducting polymers (ICPs). The ICPs contain monomers that can acquire charges through oxidation and reduction, thereby, altering the electrical conductivity [57]. The interaction of the conductive polymers with the target gas (analyte) causes a change in the carrier density and mobility, which alters the conductivity across the sensor. Figure 4 depicts a section of the p-type conducting polymer that is exposed to CO [58]. On exposure to CO, the carbon atom in CO attracts the pair of electrons from the nitrogen atom in NH, resulting in a positive charge at the nitrogen atom in the polymer structure. This charge carrier increases the conductivity across the membrane structure, thereby, increasing the overall electrical conductivity.

Besides, the usual CPC gas sensors, recent research has paved the way for fabricating CPC gas sensors with nanoparticles. This has been achieved by creating "conductive polymer nanostructures" using electrospinning that relies on the use of templates during the polymerization process [59]. CPCs and the nanoparticle-based conductive polymers have demonstrated promising results as they have been found to be more sensitive and yield a shorter response time in comparison to MoX sensors, wherein, the resistive sensors have gained popularity due to their cost-effective fabrication, smooth operation [59], good durability and environmental stability [56].

2.3 Carbon nanotube-based gas sensors

Carbon nanotubes (CNTs) and their composites have proven to be good candidates for gas sensors owing to their large surface area to volume ratio [60], leading to high sensitivity. CNTs consume low power and are deemed portable while simultaneously rendering easy miniaturization on GSAs [61]. These gas sensors can be made of either single-walled carbon nanotubes (SWCNTs) or multi-walled carbon nanotubes (MWCNTs) and can easily operate at room temperature, with relatively fast response times [11]. Akin to previous sensors, the presence of the gas is detected by measuring the change in the conductance of the nanotubes, wherein, a higher concentration of the adsorbed target gas depicts a higher change in the nanotube conductance. A visual representation of the gas sensing using CNTs is shown in Fig. 5 [62] , where the CNT is exposed to NH_3. The CNT channel connects the source and the drain electrodes as in a field-effect transistor (FET). Since NH_3 behaves as an electron donor, the adsorption process releases electrons into the CNT channel, increasing the current flow and thereby, yielding a measurable output (See Fig. 5).

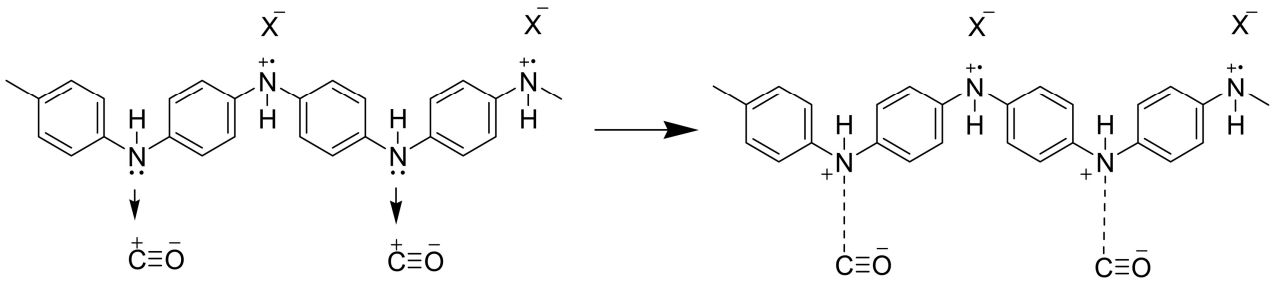

Fig. 4. Cross-section of a conductive polymer gas sensor [58].

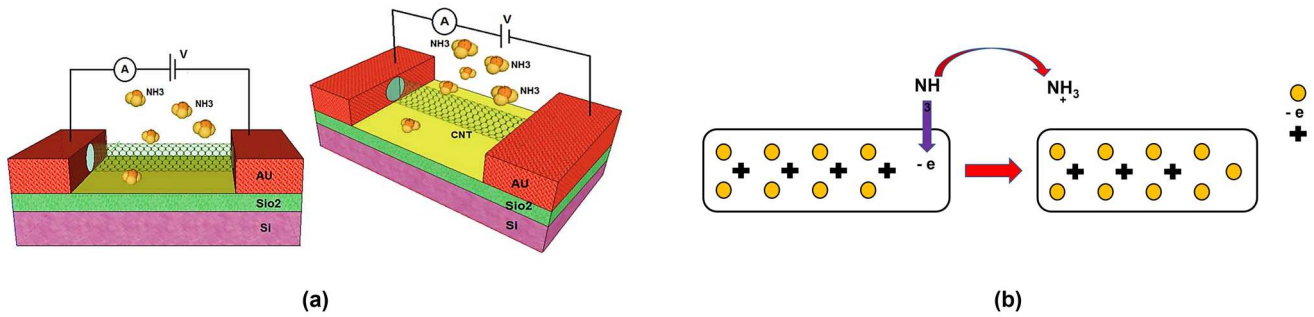

Fig. 5. a) SWCNT gas sensor, b) Working of the SWCNT gas sensor with ammonia donating an electron to increase conductivity [62].

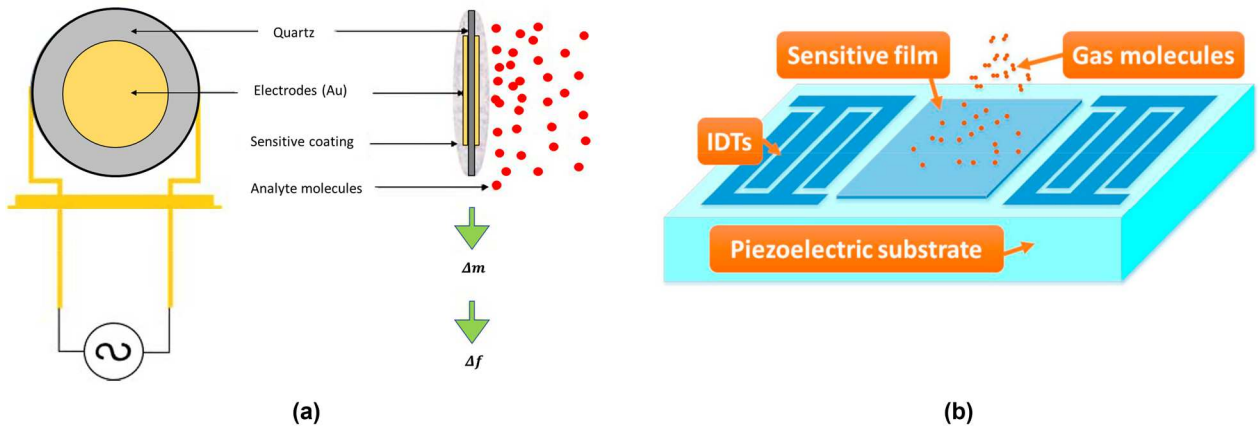

Fig. 6. a) Working principle of the QCM gas sensor. Reproduced with permission from [68], b) Working principle of the SAW gas sensor [71].

Although these sensors have high sensitivity, it can be further improved by chemical functionalization of the CNTs with functional groups [63]. For instance, Pandhi and Chandnani [60] discussed the functionalization of CNTs using groups such as COOH and OH at the surface of the CNTs to yield better performance than pure CNTs. The performance of the CNT-based gas sensors can also be enhanced through additional doping of nanoparticles on the surface of the nanotubes [63, 64] which has proven to increase the sensitivity of the CNT-based gas sensors to a particular target gas. In recent times, nano-porous silicon-based gas sensors have also claimed popularity owing to similar properties. The porous nature of the silicon offers a high surface to volume ratio akin to CNT-based sensors [65]. By providing high sensitivity, selectivity, fast response time, good repeatability while testing for benzene, butane and methane, these sensors could be a potential competition for CNT-based gas sensors [65–67].

2.4 Acoustic wave sensors

Acoustic sensors are based on two main fabrication technologies: using quartz crystal microbalance (QCM) and surface acoustic wave (SAW) [14]. For the QCM, the quartz crystal serves as the resonating element [68], wherein, the mass of the adsorbed target gas results in a change in the oscillating frequency that can be measured as the output of the sensor (See Fig. 6). This ability of the QCM-based acoustic sensors to detect a particular gas is derived from the absence of the need for charge carriers and heat; thereby, giving them an upper hand in comparison to other gas sensors [69]. Despite the remarkable performance of QCM-based acoustic sensors, their sensing capabilities have been studied further by Yang et al. [70] to highlight the fabrication of copper doped ZnO nanorods for enhancing response of these sensors.

On the other hand, the SAW sensor is based on the piezoelectric effect, wherein, the vibrating material is superimposed with thin chemically reactive layers that can adsorb the target gas [71, 72] (See Fig. 6). The reactive layers easily adsorb the gas, as a result of which, the velocity and the attenuation of the propagating wave undergoes a measurable change [73, 74]. Raj and Singh [75] studied the impact of coating different reactive layers such as ZnO, SnO_2, TeO_2 and TiO_2 on SAW-based acoustic sensors, with ZnO deposited SAW sensors demonstrating superior performance when compared to other reactive layers. The acoustic sensors are found to be sensitive to the weight of the adsorbed target gas, are compact and can respond to almost all types of gases.

For acoustic wave sensors in general, besides good reproducibility and fast response time, good selectivity is also of paramount importance in detecting the target gas, whereby, researchers have studied the use of various sensor materials for their fabrication [76]. Metal-oxide films fabricated onto SAW sensors have been deemed as highly reliable materials for improving the selectivity of acoustic sensors. This is due to the fact that MoX films help improve selectivity without compromising the wave propagation functionality of the sensor. In addition to MoX films, acoustic sensors have been designed with polymer-based sensing materials which have been discussed in Section 2.2. Based on the target gas, acoustic sensors can be coated with specific polymer materials [77], however, these materials fare lower in comparison to MoX-based layers on account of their waning stability and reproducibility over time.

2.5 Catalytic sensors

The operating principle of the catalytic gas sensor is determined by the oxidation of the target gas on the surface of the sensor, wherein the oxidation results in the release of heat, and thereby an increase in the resistance [78]. The amount of heat released due to the oxidation is directly proportional to the concentration of the target gas. Catalytic sensors are mostly used for the detection of flammable gases such as hydrogen, methane, and carbon monoxide and for gas pipeline explosion detection [14, 78]. The working principle of the catalytic sensor is demonstrated through a Wheatstone bridge circuit as shown in Fig. 7 [79]. On

exposing the sensor to the gas, the sensing element which is usually built using platinum coils results in a combustion reaction. Subsequently, the reaction causes a measurable change in the resistance, ΔR, that is directly proportional to the concentration of the exposed gas. The Wheatstone bridge converts the resistance change into an output voltage which is used to extract the gas concentration using calibration curves.

Although these sensors are continued to be widely used, they offer low sensitivity and selectivity [14], while rendering high power consumption and long response times [78]. To address the issue of high-power consumption, Brauns et al. [80, 81] proposed the fabrication of a catalytic sensor with a platinum catalyst using the MEMS technology. Consequently, this fabrication process provides catalytic sensors with faster response, high signal reproducibility and comparatively lower power consumption. Moreover, the operating temperature is proven to reduce by utilizing porous catalytic materials on the surface of the sensors that provide large surface areas and in addition, minimize the power consumption of the sensors [82].

2.6 Metal organic framework-based sensors

Metal organic frameworks (MOFs) constitute a very promising sensitive layer in comparison to other porous materials and polymers for gas sensing applications due to their high specific surface areas, tunable pore size, and easy functionalization of the organic part upon selection of different metal ions and organic bridging ligands. Furthermore, these porous materials have proven robustness and possible reuse and storage under human conditions without degradation in their performance.

Recent research studies have demonstrated the possible integration of MOF thin films on electrically-actuated microstructures to deliver accurate sensing information [83, 84]. The nature of these materials renders a large surface area in gas sensors that can be easily modified to improve the selectivity of the sensor to a particular target gas [83]. Moreover, MEMS/NEMS based resonators have been increasingly employed for the detection of low gas concentrations owing to their small size, cost effectiveness thanks to batch fabrication, and low power consumption [85]. It is important to note that the cross-sensitivity between the temperature and the target gas experienced by gas sensors adversely degrades their accuracy [86], wherein, the efforts undertaken to combat this issue resulted in a costly fabrication and higher power consumption. In recent years, researchers in [85, 86] have discussed a novel approach that utilizes a MEMS resonator coated with a MOF for sensing multiple stimuli simultaneously. The resonator is electrostatically actuated [86] and uses first and second order modes of vibration for simultaneous detection of the ambient temperature and the gas concentration (water vapor). As shown in Fig. 8, the frequency responses of the resonator near the 1st and 2nd modes are used to simultaneously measure the operating temperature and the water vapor concentration. Another remarkable approach undertaken for the detection of multiple stimuli is demonstrated in [87], where the authors proposed the design of a MEMS gas sensor using two mechanically-coupled microbeams. Capitalizing on its properties, the microbeams were coated with MOFs for the simultaneous detection of CO_2 and CH_4 using dynamic features of the microbeams. Dynamic features such as the 1st six natural frequencies, RMS of the microbeam deflection, maximum and minimum values of their deflection were used with deep neural networks to attain successful results for both classification and regression. A sketch of the MOF device, including its different layers, along with its SEM image are shown in Fig. 9.

Research studies demonstrated that the exposure to the target gas alters the amplitude of vibration and the shift in the natural frequency is linearly proportional to the gas concentration [83, 86, 88]. In addition, the proposed resonators can act as switchers when the gas concentration exceeds a certain threshold and have proven to remarkably reduce power consumption and size while simultaneously enhancing the sensitivity and selectivity of the sensor [83].

2.7 Optical sensors

Optical gas sensing technology forms an important facet of gas sensors and has found an immense number of engineering applications. Studies indicate that several gases such as NO, CO, H_2, NH_3 and H_2S, absorb infra-red or ultra-violet light of different wavelengths, which helps in their detection [39, 89–91]. Most commonly used optical sensors utilize the non-dispersive infra-red (NDIR) absorption technique using an NDIR gas sensor as shown in Fig. 10. This sensor consists of the infrared source, the dual channel detector and the optical cavity for the target gas [91]. The target gas present in the cavity reduces the intensity of the travelling light, which is then detected by the active channel [91, 92]. The active channel passes only the wavelength of the absorption band of the target gas, whereas, the remaining wavelengths are diverted to the reference channel. As a result, the light intensity detected at the active channel provides information about the presence of the gas and its concentration.

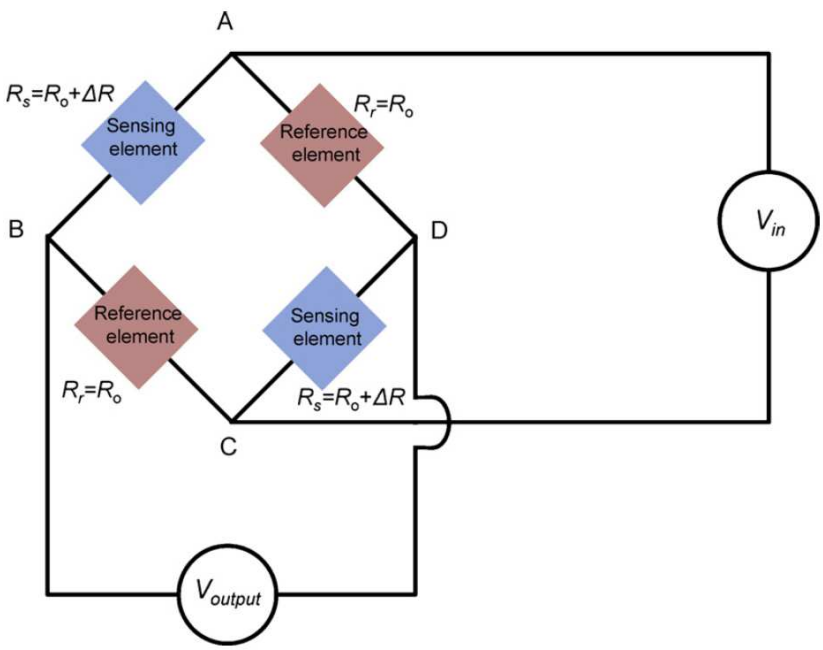

Fig. 7. Operational Wheatstone bridge circuit of a catalytic gas sensor. Reproduced with permission from [79].

Besides the NDIR absorption technique, optical gas sensors also rely on non-absorption techniques such as UVF [93] and gas chemiluminescence [94], where, the chemiluminescence process results in the emission of radiation of a particular wavelength due to the chemical reaction between the target gas and the sensor surfaces. On the other hand, the fluorescence-based gas sensors are based on the emission of light with a particular wavelength due to the excitation of the gas molecules on absorbing the radiation [95]. Optical sensors have been widely used due to their portable structure and ability to provide a non-invasive approach with good predictive accuracies [96, 97]. Using spectral analysis, Zhang et al. [98] proposed the use of optical gas sensors for detecting NO_2, SO_2, NO_2 and C_6H_6. After the interaction of the gas with the emitted light, a spectrometer was employed to collect and study the response of the light at the output. On comparing the performance of the optical sensor with a MoX sensor, it was observed that the optical sensor rendered a lower response and recovery time, thus, reiterating the remarkable performance of optical sensors for gas detection.

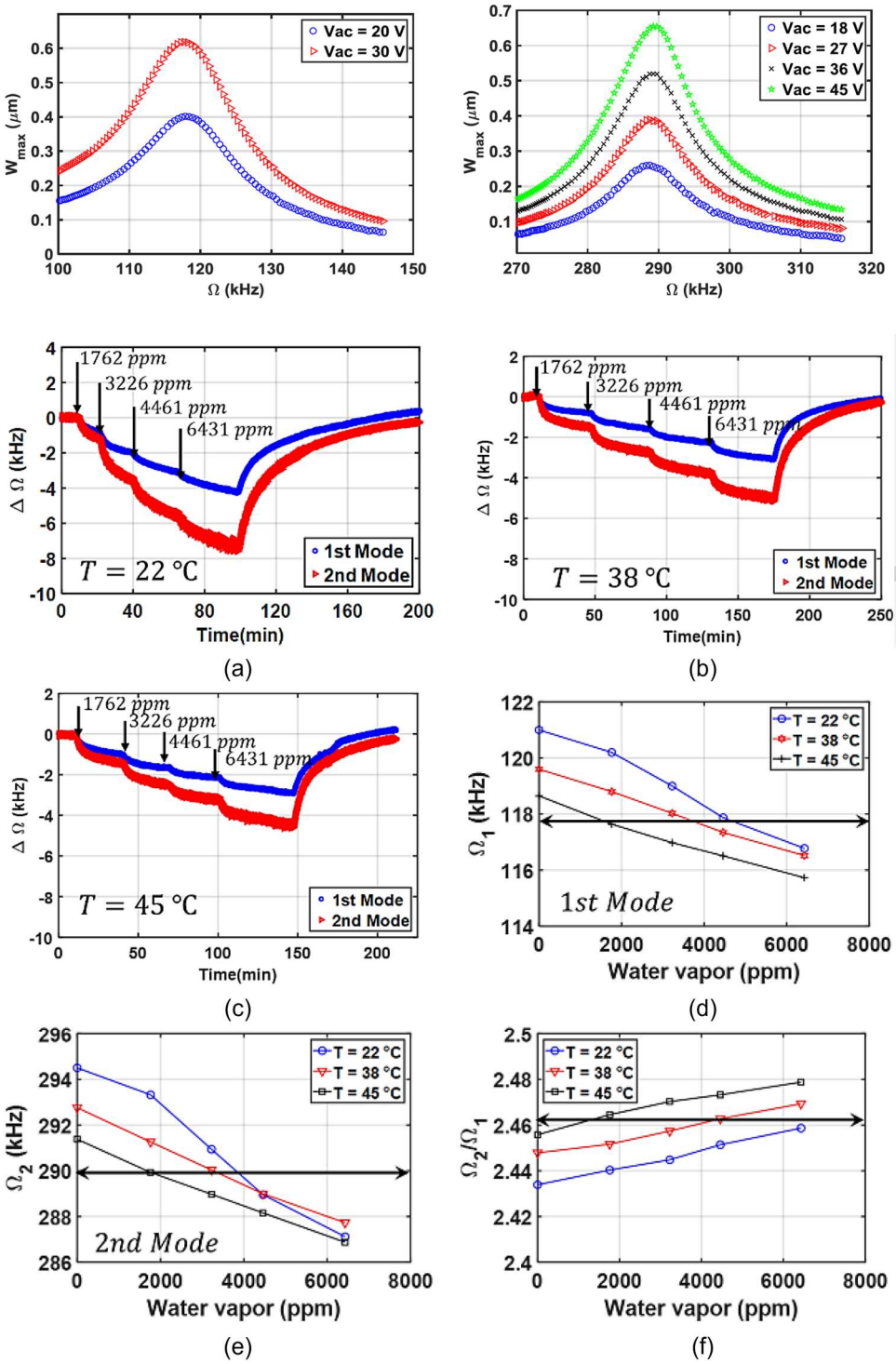

Fig. 8. a) Frequency response of MOF sensor near the 1st and 2nd modes, b) Frequency shifts detected for different water vapor concentrations near the 1st mode and 2nd mode [86] © (2018) IEEE.

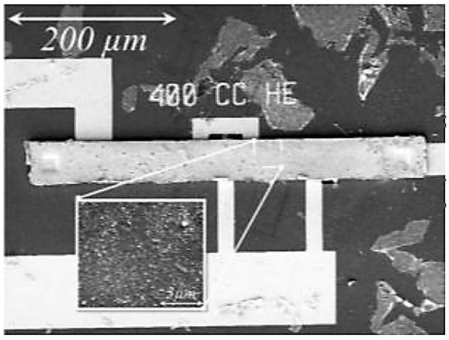

(a)

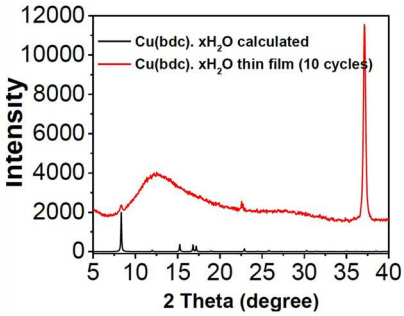

(b)

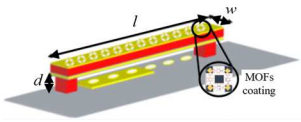

Color	Material	Thickness (nm)	Modulus of Elasticity (GPa)	Density (kg/m^3)
	Silicon Dioxide (SiO_2)	3000	85	2300
	Chrome (Cr)	50	279	7190
	Gold (Au)	200	79	19300
	Polyimide (Pi)	4300	8.5	1400

(c)

Fig. 9. (a) An SEM image of the fabricated microbeam with MOFs functionalization. (b) XRD of Cu(bdc).xH_2O MOF thin film grown on the microbeam (red) and its calculated pattern (black). (c) Schematic of the microbeam with the lower electrode perforation showing the material layer types, properties, and thicknesses [86] © (2018) IEEE.

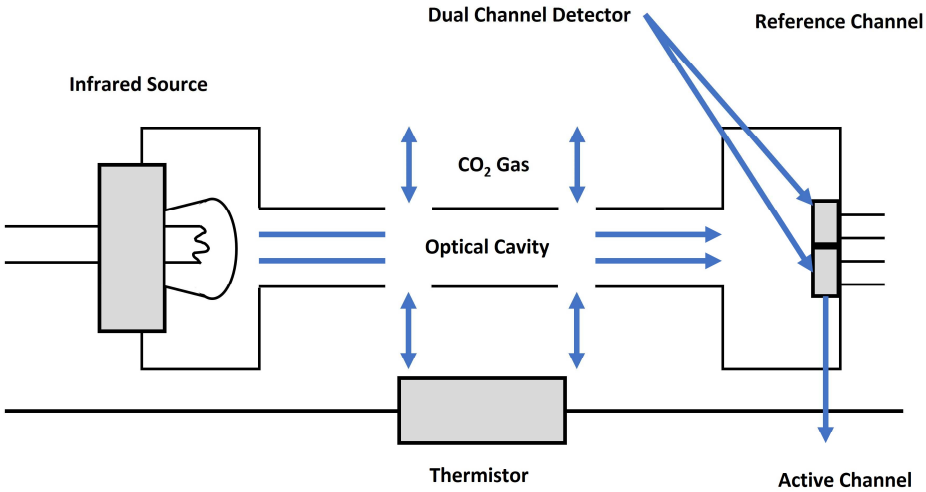

Fig. 10. Schematic of the optical sensor illustrating its operating principle [91] © (2012) IEEE.

3. Machine Learning in Gas Sensing

Besides the progressive research on the design of the E-nose using different fabrication technologies, current research trends have shown an increasing inclination towards gas sensor data analysis. The E-nose evidently offers a more lucrative advantage in comparison to single gas sensors. A single sensor effectively responds to a particular gas to produce a specific gas fingerprint, whereas, multiple sensors in the GSAs of an E-nose provide multi-dimensional response signals. These signals contribute to unique fingerprints for each gas, thereby, providing more information that can consequently be used for machine learning. As a result, the appropriate selection of the algorithms for an E-nose helps in improving its functionality and dependability over time considerably. A more detailed operation of the E-nose is depicted in Fig. 11. The vital aspects of the E-nose system operation can be simplified into three main categories: signal acquisition using the sensor arrays, signal pre-processing using feature extraction or feature selection, and modeling of machine learning algorithms which entail classification and regression [14].

3.1 E-nose operation

The signal acquired from the GSAs is based on the principle that each sensor develops a different fingerprint for each chemical compound that it detects [13, 14]. The sensor goes through a physical or chemical change depending on the sensor type, rendering a response that is unique to a gas or a particular concentration as illustrated in Fig. 12. The ability of the E-nose to correctly identify the type and concentration of a chemical compound is heavily dependent on the data retrieved from the signals. The inability to

draw significant information from the sensor signals can easily result in the ineffectual performance of the complete E-nose system [99]. As a result, signal pre-processing techniques have gained high ground, forming the backbone of E-nose systems. Since unprocessed raw senor data may suffer from high noise-to-signal ratios and drift errors [14], pre-processing techniques work towards eliminating noise and redundant data points, outliers, resampling the signal, and implementing smoothing techniques for better visualization of the signal.

Pre-processing techniques applied on large sensor datasets that help to ameliorate the robustness of the machine learning models for classification and regression, can mainly be classified into feature extraction techniques and feature selection techniques. Feature extraction and selection form a subset of dimensionality reduction techniques and are used to transform raw data into appropriate input features for machine learning algorithms [100]. In doing so, they enable to eliminate redundancy from the raw data and retain germane features that can enhance the accuracy of the machine learning models. As a result of the pre-processing, the data is organized into a format that contains the features, also referred to as *attributes*, and the *gas type* corresponding to these *attributes* is referred to as the *label* during classification, whereas, the *gas concentration* is considered the *label* during regression. Following the pre-processing, the dataset is divided into training and testing datasets for performing classification and regression as shown in Fig. 13. For practical purposes, 70-80% of the dataset is usually reserved for training, and the remaining 20-30% is used for testing [101]. The training dataset is used to build the machine learning model for both classification and regression. The class label for classification (gas type) is *categorical* whereas, the class label for regression (gas concentration) is of *numerical* type. The machine learning algorithms applied for classification and regression include the k-Nearest Neighbors (kNN) [102], Support Vector Machine (SVM) [103], Artificial Neural Networks (ANN) [104], Random Forests (RF) [105, 106] and Decision Trees (DT) [107]. The use of a single classification or regression machine learning algorithm does not provide the best prediction for the gas type and concentration. As a consequence, ensemble methods that combine various weak models or diverse models to render a final prediction are employed. In many cases, ensemble methods prove to have higher accuracy when compared to the individual classification and regression models.

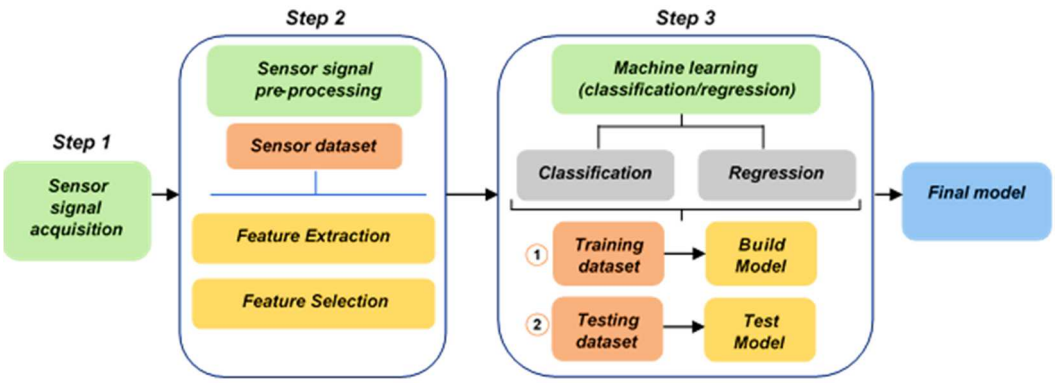

Fig. 11. Block diagram representation of the steps involved in the E-nose operation.

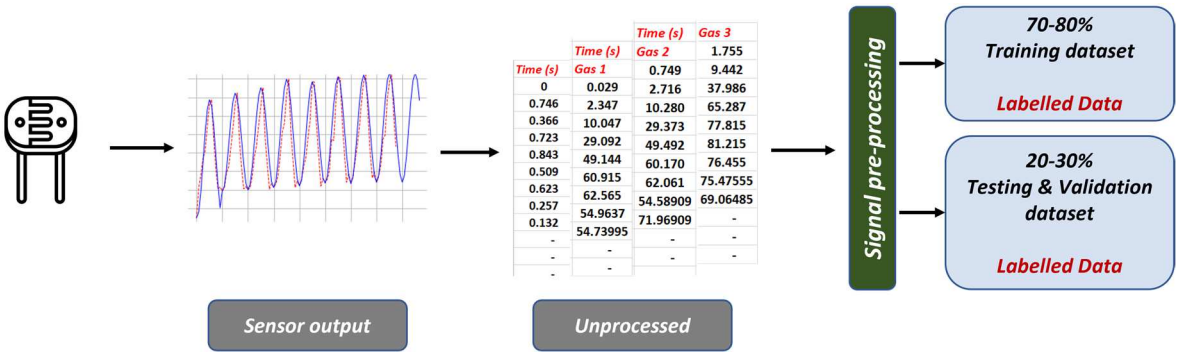

Fig. 12. Signal acquisition and processing of raw sensor data.

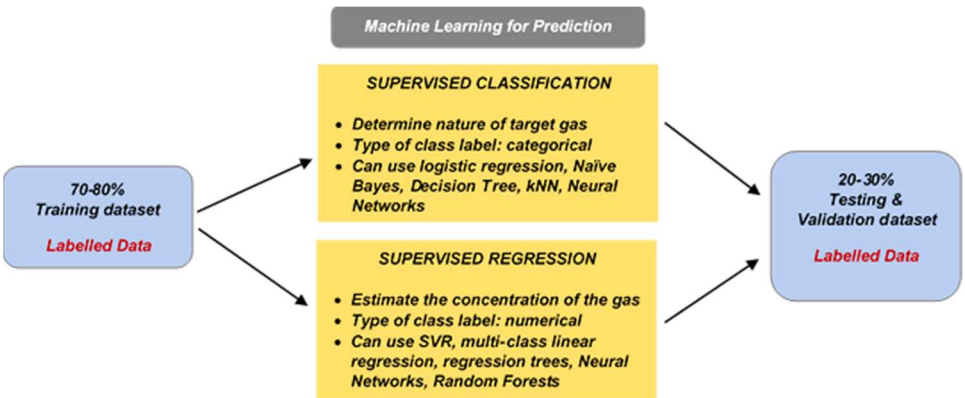

Fig. 13. Machine learning using training and testing datasets.

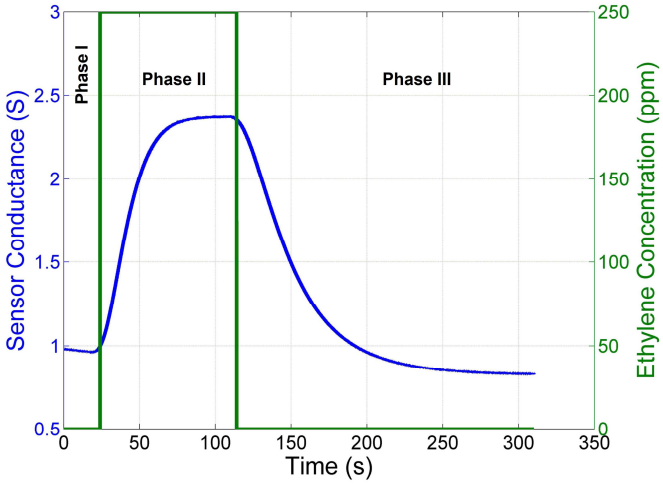

Fig. 14. Typical response of MoX gas sensor on exposure to ethylene. Adapted from [112].

3.2 Feature extraction

Transformation of the sensor raw data into features that can relay significant information [108, 109], aids in minimizing the complexity of the original data and hence, the computational complexities of the machine learning model [110]. In addition, implementation of feature extraction helps to circumvent machine learning model overfitting and provides better explicability of the data under investigation [111]. Prior to extraction, the sensor signal represents numerous data points that correspond to the adsorption and desorption phase of the gas on the surface of the gas sensing material. For instance, Fig. 14 shows the typical response of a MoX gas sensor for the detection of ethylene [112]. Clearly, the response depicts the change in conductance over time during the gas exposure with three different phases; *Phase I* (initial phase), *Phase II* (exposure phase), and *Phase III* (regeneration phase).

Irrespective of the nature of the signal, there are several kinds of feature extraction techniques that are used for E-noses. One category of techniques focuses on extracting *piece-meal features* of the signal [113]. Such features that can be extracted for different phases of operation can include sensor signal sensitivity, slope of the signal, rise time of the signal and average value of the signal [114]. On the contrary, some techniques focus on extracting steady-state and transient features [115], low-frequency and high-frequency features [116]. With this in mind, feature extraction techniques are designed to provide characteristic features that summarize a major portion of the information contained in the original raw data. To this end, feature extraction techniques tend to extract features in the transform domain using Fourier transforms or extract all signal features from the sensor response by fitting the sensor signal to a certain response curve [113]. Amongst the feature extraction techniques are also those which provide a completely new set of features through the transformation of the original dataset. A major drawback associated with these techniques is the inability of the new features to render useful information about the original features, thereby, making it hard to interpret the new features [117]. Thus, it is critical to select the appropriate method to extract pertinent features that can represent the sensor response to the target gas in order to improve the performance of classification and regression. Table 2 summarizes the main techniques used for feature extraction. These feature extraction techniques are discussed in further detail below [118-122].

3.2.1 Principal component analysis

Principal Component Analysis (PCA) is an unsupervised feature extraction technique, sometimes used for clustering/classification, that extracts the most relevant information from the original dataset through a linear transformation of the data [123]. PCA exploits the correlation between the data points, i.e., it attempts to find the combination of input features that best represents the original feature set while simultaneously reducing the data dimensionality. This results in the formation of new uncorrelated values known as *principal components (PC)*, where an *n-dimensional* dataset results in *n* principal components. The principal components attained using eigenvectors and eigenvalues are independent, orthogonal, linear combinations of the original variables in addition to being uncorrelated [109]. These PCs allow for the reduction in redundancy while simultaneously maximizing the variance associated with the feature dataset as shown in Fig. 15 [124]. PCA then aligns the original dataset along the direction of the new PCs by retaining the PCs with the highest variance. For instance, in Fig. 15, it is observed that the PC1 (red) renders the highest data variance when compared to PC2 (green) based on the sparse arrangement of the data points along its direction.

Table 2. Summary of feature extraction techniques.

Technique	Technique Type	Characteristics	Reference
PCA	Unsupervised	Unsupervised and hence does not consider labeled data Aims to find the principal components that maximize the variance between the data Assumes a linear relationship between the input and the output variable Offers kernel-PCA that deals with non-linear data	[118, 119]
LDA	Supervised	Supervised technique that uses labeled data Aims to find the linear discriminants that maximize separation between different classes Assumes a linear relationship between the input and the output variable Assumes the data follows a Gaussian distribution	[120, 121]
ICA	Unsupervised	Unsupervised technique that caters to a mixture of signal data Aims to find independent components from the data and eliminate redundant noise Offers a linear dimensionality technique that assumes the data to be Gaussian	[122]

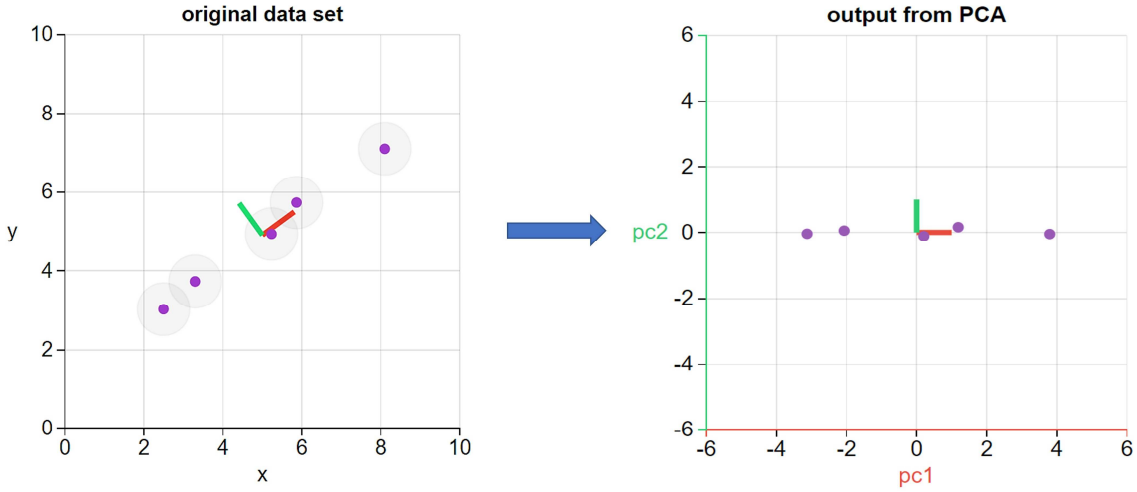

Fig. 15. Transformation of original dataset along new axes of PCs using PCA [124].

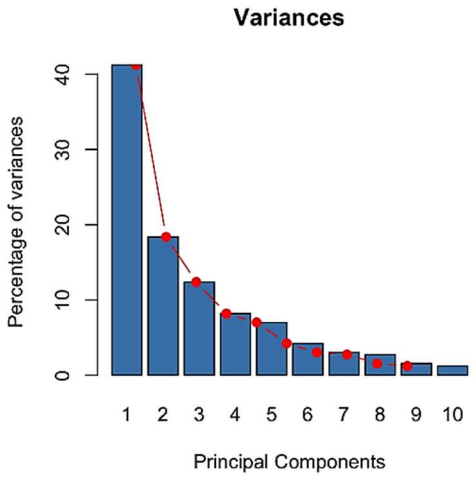

Fig. 16. Visual representation of decreasing variance from PCs [125].

The amount of variance offered by each principal component can be easily visualized through a scree plot, as displayed in Fig. 16 [125]. In most cases, the first three principal components, *PC1*, *PC2* and *PC3* tend to depict the highest variance by capturing the highest percentage of the information from all the features present in the dataset. PCA deals with linear data, whereas an extension of PCA, referred to kernel based PCA deals with data that show non-linear behavior. Kernel PCA uses kernel tricks that use higher dimensions for the non-linear mapping of the data, following which the decision boundary for maximizing the variance between the classes becomes linear [126].

3.2.2 Linear discriminant analysis

On the other hand, Linear Discriminant Analysis (LDA) is a supervised feature extraction technique that uses labelled data to maximize the difference between the various classes [14]. LDA, widely used for feature extraction as well as classification, renders a linear transformation of the data to minimize the dimensionality and maximize the discrimination between the different classes [127]. Akin to PCA, the main purpose of LDA is to minimize the spread/variance between points within a class while maximizing the distance between the means of each class, therefore, working to minimize intragroup distance and maximize intergroup distance as illustrated in Fig. 17 [128]. It can be seen that a good projection in comparison to a bad projection entails maximum separation between the means of the two classes, thereby, resulting in a good and distinct separation of the classes. However, this class separation may not always be possible which results in one of the shortcomings of LDA. In cases where the classes are not linearly separable, LDA may not be able to discriminate between the two classes. Nevertheless, the easy interpretation and simple implementation of LDA makes it a viable option for robust classification problems.

3.2.3 Independent component analysis

Independent Component Analysis (ICA) is another linear-based dimensionality reduction akin to PCA that performs linear transformation of the original dataset [129]. The result of the linear combination is referred as to an independent component that disregards any anomaly or noise within the data. Moreover, the ICA technique is more commonly utilized in the biomedical field as discussed in [130]. ICA has also been implemented for blind source separation (BSS), that refers to the extraction of independent sources from a mixture of medical signals. This allows for the applications of EEG and ECG to extract and reliably separate useful signals from noisy signals. Therefore, depending on the nature of the data and the requirements of the application of interest, PCA, LDA or ICA can be effectively implemented to retain representative features from the sensor response.

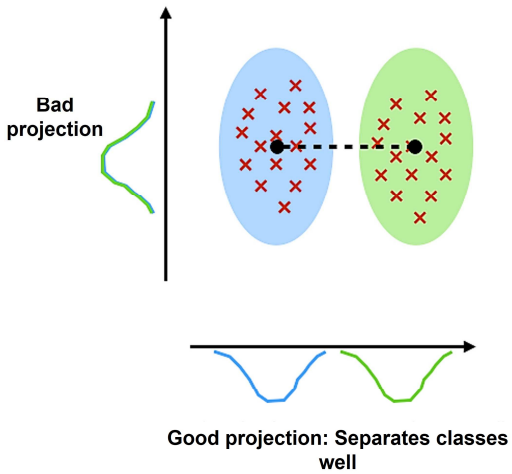

Fig. 17. Class separation using LDA [128].

3.3 Feature selection

Feature selection techniques select a subset of representative features from the complete dataset that provides maximum contribution to the prediction of the desired output. Over the last few years, these techniques have been undertaken to provide agile machine learning models which render higher prediction accuracies. The prime objectives of feature selection are to avoid model overfitting and improve the machine learning model performance; offer fast and reliable performing models; and provide a deeper insight into the data generation process [131]. As a result, feature selection techniques are demarcated into several categories based on certain criteria including [132]:

- The type of training data: they are divided into supervised [133, 134], unsupervised [135, 136], and semi supervised [137] feature selection models.
- Their interaction with the machine learning models: they are divided into filter, wrapper and embedded methods.
- The searching strategies: they are divided into sequential, randomized and hybrid methods.
- The evaluation criteria: they can be used based on correlation or distance measures [100, 109].
- The type of the output: they are demarcated into feature rank and subset selection models.

Given the type of training data, supervised techniques select features using datasets that contain class labels, whereas, unsupervised techniques use unlabeled datasets to select features. Semi-supervised techniques, on the contrary, use both labeled and unlabeled datasets. For the purpose of gas sensing, the machine learning algorithms primarily follow the supervised path, thereby, leading to the implementation of supervised feature selection, which establishes a relationship between the features and the class label. Regardless of the technique being implemented, Ang and Mirzal divided feature subsets into four main categories: i) “irrelevant and noisy features”, ii) “weakly relevant and redundant features”, iii) “weakly relevant and non-redundant features” and iv) “strongly relevant features” [138]. Consequently, the selection of strong relevant and less redundant features demonstrates the capability to ameliorate prediction performance while minimizing computational complexities.

Furthermore, supervised techniques can be classified into filter, wrapper, and embedded methods [139]. Filter methods estimate the relevance and select features based on their intrinsic characteristics using metrics such as Mahalanobis distance, Euclidean distance, correlation, and Chi-square. In several cases, the features are finalized based on a relevance score, where the features with the lowest scores are not taken into consideration. On the other hand, wrapper methods are usually combined with the machine learning algorithms. Instead of pre-selecting a subset of features, wrapper methods select the relevant features by considering their accuracy when applied to the machine learning algorithm. Two most commonly used wrapper-based feature selection methods are the Sequential Forward Selection (SFS) and the Sequential Backward Elimination (SBE). The SFS begins with an empty set and continues to iteratively add the features that improve the algorithm performance [109]. In other words, it provides the greatest increase in the predictor performance [140]. The SBE, on the other hand, begins with the complete set of features and iteratively eliminates features that affect the algorithm performance.

Finally, embedded methods capitalize on the advantages of both, the filter, and the wrapper methods. Akin to wrapper methods, embedded methods also interact with the machine learning algorithm and, in many cases, contain built-in feature selection. The embedded methods provide a way to perform feature selection and model training simultaneously [139]. This is further corroborated in [141], which attributes this characteristic of embedded methods to their inability to separate feature selection and the model training process. As a result, in comparison to filter methods, embedded methods work alongside the machine learning algorithm and offer a quicker way of selecting the features, in contrast to wrapper methods. Popular embedded feature selection techniques include RF, Ridge regression and LASSO that have built-in techniques that pre-process the data and render the appropriate feature subset for the machine learning algorithm. Table 3 provides a list of different feature selection techniques and their characteristics [142-144].

3.4 Machine learning algorithms

For gas sensing, the two main characteristics of the gas to be determined are: 1) the gas type using classification and 2) the gas concentration using regression. Several machine learning techniques used for these tasks are discussed in detail below.

3.4.1 k-Nearest neighbors

The kNN algorithm is deemed a traditional and simple non-linear classification algorithm that uses distance metrics to classify data samples. The two main parameters of this algorithm are k and the *distance metric* [145]. The working principle of this algorithm is illustrated in Fig. 18 which shows how the classification of a new data sample is achieved. Given by its name, kNN attempts to find the k nearest neighbors of the new data sample and allocates a label to it through majority voting. As shown in Fig. 18, using a distance metric such as Euclidean distance, nearest k neighbors are represented by $Num(d_i)$ within a localized region and the similarity between all the data samples within the region is determined. As a result, any new data point d_i, that falls within that local region is assigned the label based on the similarity obtained through majority voting. Given its ease of implementation, the kNN algorithm can be deployed for multi-class classification problems, rendering low misclassification errors [146].

Table 3. Feature selection technique and their characteristics.

Technique	Characteristics	Examples	Reference
Filter methods	Works independent of the machine learning algorithm Provides fast computation and low computational cost Can be further divided into univariate and multivariate methods Univariate methods ignore feature dependencies, resulting in lower performance when compared to multivariate methods Multivariate methods are slower than univariate methods but provide feature dependencies	Mahalanobis distance Euclidean distance Correlation Chi-square Information Gain Gini Index	[109, 142–144]
Wrapper methods	Works in collaboration with the machine learning algorithm Uses feature dependencies to in the feature selection process Computationally more intensive than filter methods	SFS SBE	[108, 137, 142]
Ensemble methods	Works in tandem with the machine learning algorithm Offers better computational efficiency in comparison to wrapper methods	RF Ridge regression LASSO	[109, 139, 141]

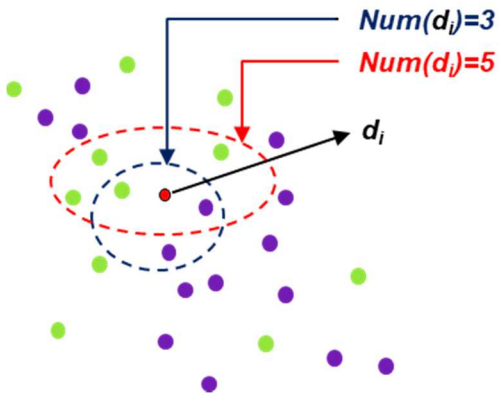

Fig. 18. Working principle of the kNN algorithm.

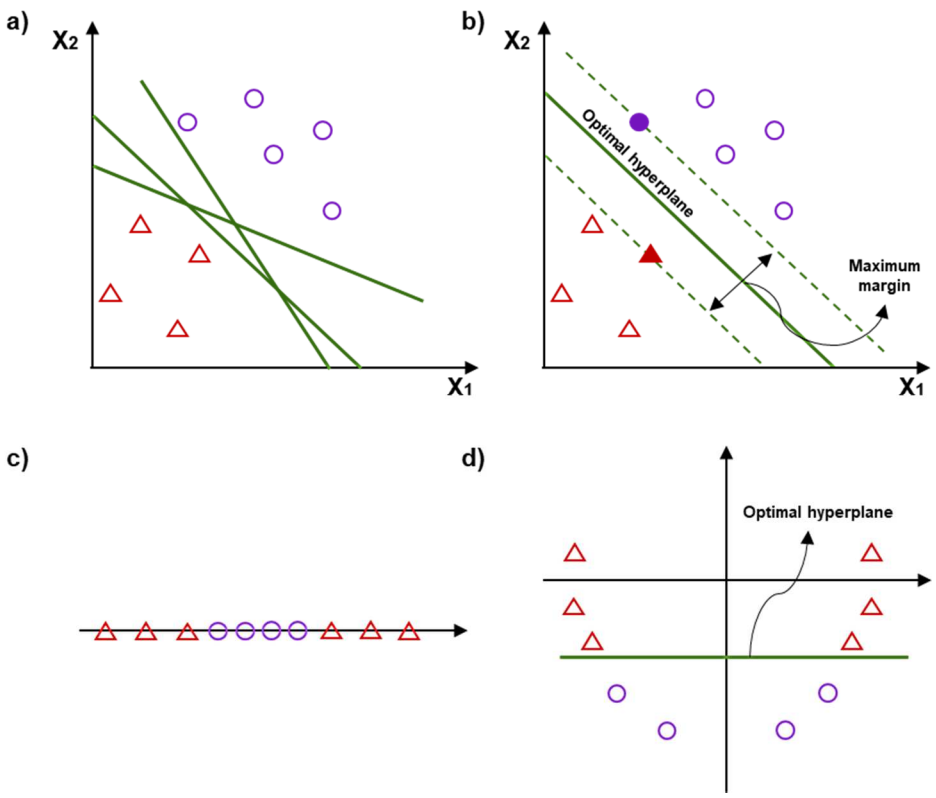

Fig. 19. Working principle of the SVM algorithm: a) Multiple hyperplanes for class separation, b) Optimal hyperplane with maximum margin, c) Linear separable class, d) Use of kernels for linear separation. Adapted with permission from [148].

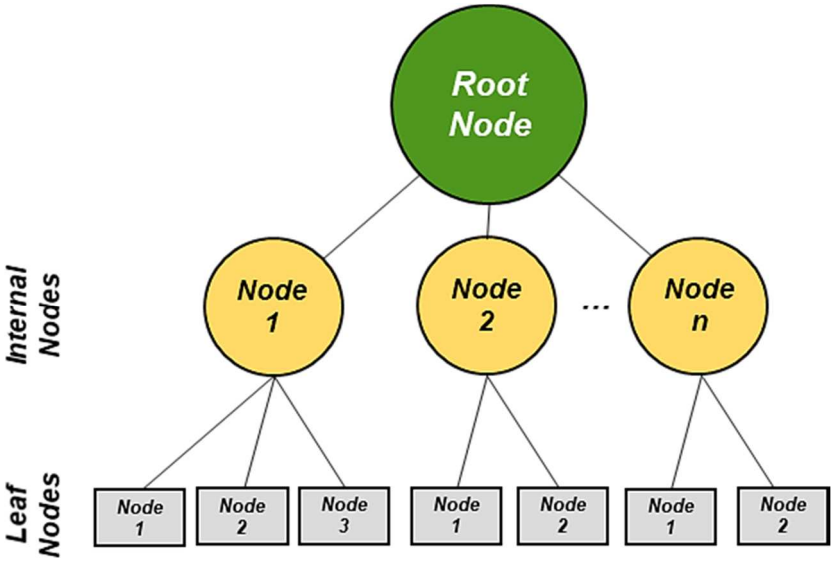

Fig. 20. Working principle of the DT algorithm.

3.4.2 Support Vector Machine

Support Vector Machine (SVM) is an algorithm that is most commonly used for solving binary linear classification problems using support vectors [147]. However, SVM can also be used to for multiclassification problems which are contrary to one-to-one classification. The prime objective of the SVM algorithm is to determine the hyperplane that can easily classify the data points for an *n-dimensional* dataset. For a given dataset with *n* features, there are several hyperplanes that can separate the different classes as shown in Fig. 19. The most optimal hyperplane is defined as the one that provides maximum separation between the data points of both the classes. It is important to note that the SVM algorithm attempts to separate the dataset using an *(n-1)* dimensional hyperplane [148]. As a result, the hyperplane for a two-dimensional dataset is a line, whereas the hyperplane for a three-dimensional dataset is a two-dimensional plane. Support vectors are data points that are closest to the hyperplane and this can be seen in Fig. 19. The largest separation, also known as the maximum margin, is taken as the distance between the support vectors of the two classes.

In cases where a distinct segregation cannot be achieved due to noisy data, the SVM algorithm develops the hyperplane by allowing for some misclassifications errors as shown in Fig. 19. In this case, SVM aims to develop the hyperplane that equalizes both the margin and the sum of the misclassification errors. Finally, for linearly separable classes (See Fig. 19), SVM uses kernel function to transform the data into higher dimensionality which then makes the support vectors linearly separable using a linear hyperplane [147].

3.4.3 Decision Trees and Random Forests

Decision tree (DT), that is used for both classification and regression tasks, deploys a tree-like hierarchical structure [149]. As shown in Fig. 20, the highest node in the tree that represents the complete dataset is referred to as the main node or the *root node*. It is from the root node that the tree splits into different branches resulting in *n-internal nodes* [150]. As illustrated in Fig. 20, each internal node can be split further, wherein the decision to split a node is based on a *splitting criterion,* the most widely used is the *gini index*. Once the leaf node is attained, the splitting is terminated, rendering a complete tree-like decision making structure. On the other hand, RFs form another classification and regression technique that is derived from DTs. As the name suggests, in this algorithm, the complete original dataset is randomly sampled into *n-subsets* to be trained using a DT [149]. Using *n-DTs* the final result outcome is determined using majority voting (classification) or averaging (regression). Though the training data for each tree is reduced significantly, random sample subsets allow each DT to be trained on uncorrelated data, hence improving the functionality and efficiency of the algorithm.

3.4.4 Artificial Neural Networks

Artificial Neural Networks (ANN) forms a significant branch of machine learning and can be employed for classification and regression tasks. They work using multiple interconnected nodes which are activated by *activation functions* and assigned *weights* accordingly [151]. The two commonly used ANNs are the back-propagation neural network (BPNN) and the feed-forward neural network (FNN). The FNN consists of the input layers, hidden layers and the output layer as illustrated in Fig. 21 [152]. The inputs to the FNN are represented by $x(i)$, which propagate forward through the *hidden layers* in the neural network. As mentioned earlier, each node henceforth, is activated and assigned a certain weight, $w_{i/j}$ using a mathematical transfer (activation) function, $F(x)$. This function is usually a linear combination of the values coming from the previous nodes at that particular neuron [153]. The most widely used activation function is the *sigmoid function* which propagates the data up to the output layer to generate results for classification or regression. It is important to note that the complexity of any ANN is highly dependent on the number of hidden layers, the number of neurons/nodes and the type of activation function being used [153, 154]. As a result, the predictive capability of the ANN can be improved by increasing the number of hidden layers or the number of neurons. Despite having a similar framework, BPNN provides a slightly different approach. After the data is propagated forward in BPNN, the results at the output are measured with an error function that compares the results to the original values [155]. The errors are back-propagated to determine the error rendered by each node. This allows the algorithm to automatically re-adjust the weights to minimize the error and attain convergence at the output node [153].

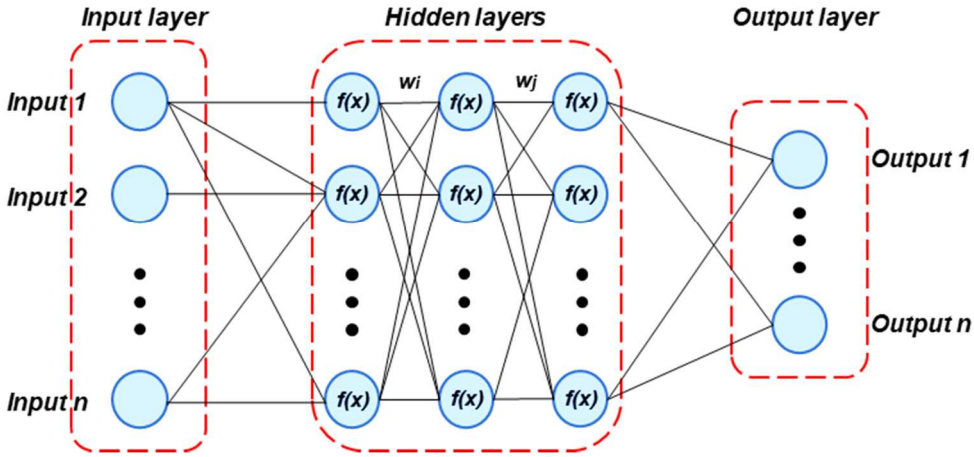

Fig. 21. Working principle of the ANN algorithm. Adapted with permission from [152].

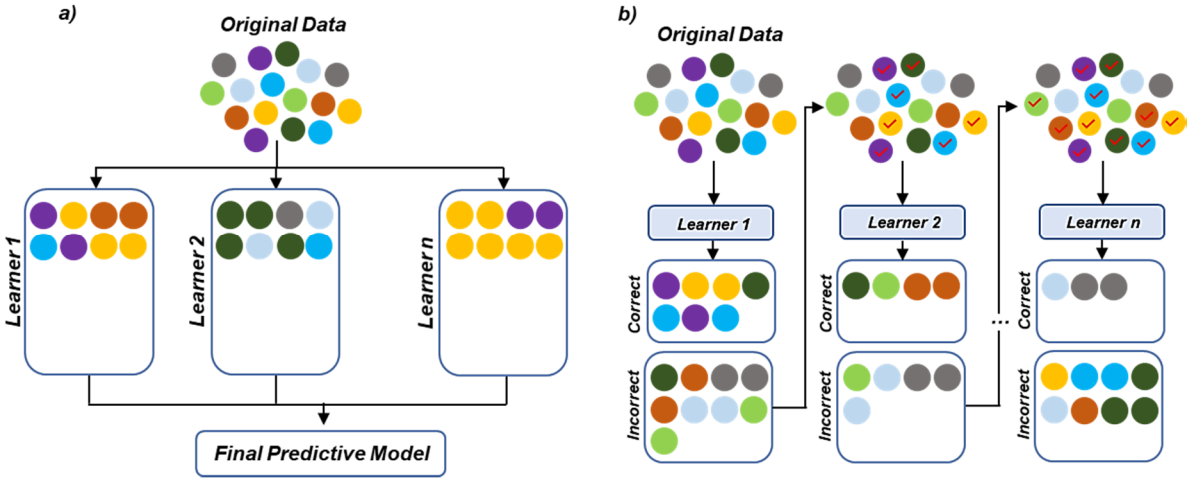

Fig. 22. Working principles of ensemble techniques: a) the bagging technique, b) the boosting technique.

3.4.5 Ensemble techniques

The ensemble techniques combine several machine-learning models to obtain the final predictive model [156]. Each machine learning model used within the ensemble is referred to as a base learner, and consequently, multiple base learners contribute to the final model. Over the last few years, ensemble techniques have shown promising outcomes in comparison to individual machine learning models for performing machine-learning tasks. The superiority of their performance is attributed to their working principle, wherein, the techniques combine distinct and weak base learners [157, 158]. The diversity of the base learners' results allows the technique to combine information from different learners and produce the final output. The two main types of ensemble techniques include the bagging and boosting [156]. As shown in Fig. 22, bagging generates random subsets of the original dataset with replacement which are subsequently trained using multiple machine learning models in a parallel manner [159]. Finally, the outcome of the ensemble is determined through majority voting (classification) or mean average (regression) of the individual learner outcomes. On the contrary, boosting provides a different approach and also enhances the predictive capability of the individual learners. Akin to bagging, boosting also generates random subsets which are trained using different learners, albeit, in a sequential manner [156, 159], where each subsequent learner is trained with a previous batch of wrongly predicted data samples. However, boosting takes advantage of these errors and assigns them higher weights to improve the accuracy of the subsequent learners in predicting them correctly (see Fig. 22).

3.5 Machine learning software tools

The machine learning techniques presented so far, play a pivotal role within an E-nose system, and thus, their implementation on machine learning platforms for E-nose applications have been profusely discussed in the literature. For instance, TensorFlow, an open-source platform provides an easy access portal for building and training machine learning models [160]. The Keras package in TensorFlow using python is widely used to implement neural network models to perform classification [161, 162] and regression [163, 164]. Other tools that use python are the sci-kit learn and PyTorch [165]. PyTorch offers an end-to-end machine learning framework [166] whereas, the scikit learn library contains numerous tools for machine learning tasks [167]. MATLAB is another popular software that has been deployed for machine learning, in addition to being used for signal generation and signal pre-processing [168–170]. Besides python, machine learning using Java is provided by Weka, a ready-to-use platform that provides different machine learning algorithms to perform data pre-processing and machine learning [171]. Graphical User Interface (GUI) platforms like the Java-based RapidMiner [172] and KNIME [173] provide the drag and drop feature for machine learning without the extensive use of programming. Over time, platforms supporting various languages in an Integrated Development Environment (IDE) led to the inception of Shogun [174]. The Shogun software was initially implemented using the C++ language and has since then been developed to support languages like python and R as well, to provide large-scale learning and an easy interface experience.

4. Practical Gas Sensing Applications of E-nose Systems

Owing to their strong capabilities, E-nose systems have been used in several applications to analyze different gases. After acquiring the sensor signal that represents a physical change in the sensor on exposure to gas, features are extracted to yield well-defined feature datasets. These datasets are then used in collaboration with machine learning algorithms to perform classification or regression tasks. Gas sensing is implemented mainly in areas of environmental management, health management and food quality control. Machine learning associated with these three arenas is discussed below. A summary of different E-nose systems used for various applications is shown in Table 4, which lists the sensor type, the machine-learning task and the sensing application [175-201]. Jasinski et al. [176] discussed the use of sensors in detecting varying concentrations of gases, namely, CO, NO_2, O_3 and SO_2, to allow for improved monitoring of the environment. Their study focused on both, the semiconductor and amperometric sensors to analyze the difference in their performance when used alongside the SVM and the Partial Least Squares (PLS) regression techniques. The data was collected over a period of 6 days, rendering 274 observations for training and 412 observations for validation, providing an extensive dataset for the machine learning approaches. Results indicated that semiconductor sensors offered better predictability when used with SVM regression, whereas amperometric sensors showed similar performance using PLS regression. The low drift and high recovery time of amperometric sensors, enhanced their capability in predicting gas concentrations. However, Jasinski et al. [176] reiterated the significance of using multiple sensors within a GSA to obtain the lowest possible gas concentration prediction errors.

Additionally, the SVR technique was used in combination with MoX sensors to detect the presence of VOCs in dynamic environments [177, 192]. Jha et al. [177] demonstrated the use of polymers in tandem with MoX sensors to improve selectivity of the sensors towards the VOCs (acetone, benzene, ethanol, pentanal, propenoic acid) during the experiment. To highlight the complexity and the superiority of the SVR technique in estimating the gas concentrations, the authors provided a comparison between various SVR approaches, with radial and polynomial kernel-based methods rendering superlative results. In most cases, using these approaches, the relationship between the actual and the predicted concentrations was almost ideal with the regression coefficient, R^2 very close to 1. This indicated superior predictive capabilities.

Besides regression, MoX sensors have been employed for classification of VOCs, proving their expertise in the field of food quality control, health and environment management. To study the potential of ANN, LDA, SVM and PLS with regards to classification, Ghanem-Varnamhasti et al. [190] used a series of MoX sensors to segregate different types of cheese on the basis of their ageing. The experiment was carried out on three different days of storage to analyze the impact of storage days on the classification of cheese. ANN rendered the highest accuracy in classifying the different types of cheese, closely followed by LDA and SVM with accuracies approximating 89% and 94% respectively. In another study, Capone et al. [197] utilized a GSA made of 5 SnO_2 sensors to detect the rancidity level of milk. The experiment was conducted over the course of eight days, with measurements recorded each day. Using the PCA algorithm and a 3-dimensional approach using the 1st three principal components, the rancidity of milk was discriminated into different categories of days with different rancidity values. The results indicated a robust correlation between rancidity levels of milk and its level of ageing. The study demonstrated a promising approach towards monitoring the quality of milk and products alike in a dynamic manner at various stages of their processing.

In areas of health management, polymer composite sensors have proven successful in detecting the presence of asthma through breath-print analysis. Dragonieri et al. [186] recorded the change in resistance across 32 polymer composite sensors that collected breath samples from a group of 40 non-smoking adults to study the presence of asthma. Using PCA, dataset was refined to include data points that provided the largest variance in the data and improved the classification accuracy. Results from the study indicated that PCA coupled with the selection of factors that offer a high variance, can provide a clear distinction between individuals with asthma and healthy individuals. Consequently, the study of VOCs in exhaled breath showed a strong potential in exhibiting signs of asthma or other respiratory diseases. Furthermore, techniques of feature selection have also shown immense capability in improving the performance of classification algorithms. Maout et al. [195] demonstrated this by coupling Recursive Feature Selection (RFE) with SVM to classify ammonia levels in breath samples that could suggest potential kidney disease. An 85% classification accuracy using SVM was improved to 91% using RFE, by eliminating the least important feature in each iteration until the best features remained.

A novel application that relies on gas mixtures as opposed to individual gas variants has been studied by Javed et al. [200, 201]. To circumvent the need for several sensors to detect gases within a mixture, Javed et al. [200] employed a GSA consisting of four mixed-potential electrochemical sensors to identify the presence of gases such as NH_3, NO_x and C_3H_8 when present as part of a mixture. The four sensors were exposed to various mixtures, wherein, each mixture was either a two-gas, three-gas or four-gas combination with varying gas concentrations. Therefore, the study involved 12 distinct gas mixtures with concentrations ranging from 0ppm to 1100ppm, subject to the type of gas. Owing to the working principle of the sensors, the dataset comprised of voltage readings that depended on the redox reaction of the gas with the surface of the sensor electrode [201], which were then used to perform classification and regression. Using a kernel-based SVM approach, multi-class classification of the dataset resulted in the determination of the gas-types present in the mixture with accuracies tending to ~95%, followed by a Gaussian-based regression approach to quantify the concentration of the gases present with errors less than ~10%. In addition to astounding results, the study highlighted vital takeaways, which suggested the great potential of SVM and Gaussian-based regression models when applied to other gas-sensor datasets as well.

4.1 Environmental management

Over the last few decades, E-nose systems have gained immense traction by monitoring VOCs such as methane, carbon monoxide, nitrous-oxide [202] and its derivatives, hydrogen sulfide, mercury, and heavy metals (in air) [203]. These systems have relentlessly focused on detecting hazardous VOCs for abating their detrimental environmental impacts. As a result, the different categories of environmental management extend to air quality control [204], water quality control [175], and monitoring of pollution [176].

Reinforcing the importance of environmental pollution monitoring, Moufid et al. [205] monitored and studied the air quality within the Meknes city of Morocco. Air quality monitoring was conducted at five areas such as the municipal solid waste landfill, regular districts, and an industrial water discharge site. Using six SnO_2 gas sensors, gases such methane, ammonia, benzene, hydrogen and carbon monoxide of varying concentrations were detected to be used for feature extraction and classification. Based on the changing electrical conductance obtained from the sensors, three features, namely conductance difference, slope of the sensor response between 10% and 90% of the exposure region and the area between the 10% and 90% of the exposure region were extracted. Results of classification using Discriminant Function Analysis (DFA) indicated excellent classification for all the gases detected at different sites (See Fig. 23). With 90% of the data variance, the E-nose system was capable of identifying and clustering gases from different sites with an accuracy of 100%. In addition, to implement Partial Least Square (PLS) regression [206] for the concentration estimation of the eight VOCs in the study, Moufid et al. [205] used the area under peaks from the sensor responses.

This rendered a high correlation coefficient of 0.97 as shown in Fig. 24, implying the strong predictive ability of the E-nose system using the PLS model.

Besides using classical MoX sensors for monitoring urban pollution, Lei et al. [207] proposed the use of a fluorescent GSA with the sensing element having a fluorescent effect, for the detection of different ammonia concentrations (*30ppb,80ppb,130ppb,* and*180ppb*). These sensors are capable of producing a fluorescent gas fingerprint from the emission spectrum obtained on the exposure to ammonia. Given the significance of feature extraction within the E-nose system operation, the emission spectra were used to extract eleven features (3 conventional, 8 microscopic) for each measurement, allowing for a holistic representation of the sensor response. Using PCA that rendered a data variance of almost *93%*, the four different ammonia concentrations were clustered distinctly to provide a high classification accuracy when detected in urban settings. Several studies have discussed the diabolical effects of prolonged exposure to ammonia in both urban and rural settings, posing adverse respiratory problems [208]. Research discussing the real-time detection of ammonia has focused on improving gas sensor fabrication to detect low concentrations of ammonia accurately [209]. Being a potent biomarker, ammonia even in low concentrations has the capability of impairing individuals' health. To account for this, Liao et al. [209] presented the design of a double layer metal-oxide gas sensor, in this case WO_3/SnO_2 for the detection of ammonia levels. In addition, they also proposed the use of MEMS microheaters in the sensing layer to simultaneously minimize the power consumption and reduce the response time [210, 211]. Consequently, keeping in mind the dire need to account for detecting ammonia concentrations at all levels, the proposed double-layer sensor design proved to be more favorable in comparison to a single-layer SnO_2 sensor.

Table 4. Summary of the different sensing applications of E-nose systems.

Application	Area	Sensor type	ML Task	ML technique	Reference
Determine water quality for shrimp farming	E	MoX sensor	Classification	LDA	[175]
Monitor environmental pollution due to gases (CO, NO_2, O_3, SO_2)	E	Semiconductor & Amperometric sensor	Regression	PLS, SVM	[176]
Quantify chemical vapor concentrations	E	MoX sensor	Regression	LS,SVR	[177]
Detect chronic pulmonary disease based on breath-prints	H	Polymer composite sensor (carbon-black)	Classification	PCA, CDA, SVM	[178]
Discriminate between different VOCs (acetone, ethanol, formaldehyde)	E	MoX sensor	Classification	PCA	[179]
Assess quality of indoor air in living environment	E	MoX sensor	Regression	BPNN	[4]
Discriminate meat samples based on mineral content	F	MoX sensor	Classification	LDA	[180]
Identify biodiesel mixtures	E	MoX sensor	Classification	LDA, QDA, SVM	[181]
Detect lung cancer using samples from healthy and lung-cancer patients	H	MoX sensor	Classification	kNN, SVM, PCA	[182]
Differentiate between healthy individuals, patients with lung cancer and benign pulmonary disease	H	MoX sensor	Classification	PCA, SVM, Naïve Bayes, LogitBoost	[183]
Distinguish benzene exposed workers with control group for early detection of health hazards	H	MoX sensor	Classification	PCA	[184]
Identify academic stress or relaxation based on VOC released from skin	H	MoX sensor	Classification	kNN, SVM, LDAC	[185]
Discriminate patients of asthma from healthy individuals and differentiate between varying degrees of the disease	H	Polymer composite sensor (carbon-black)	Classification	PCA	[186]
Identify chronic kidney disease (CKD) and different stages of CKD	H	Gold nanoparticle sensor	Classification	SVM	[187]
Differentiate between fresh, half-contaminated and fully contaminated broccoli samples	F	Chemiresistive sensor	Classification	Centroid-link cluster analysis, complete-link cluster analysis	[188]
Predict level of contamination due to pesticide residue in tea samples	F	MoX sensor	Regression	SVM, ANN	[189]
Classify different types of cheese made from different milk	F	MoX sensor	Classification	ANN, SVM, PLS, LDA	[190]
Determine fish freshness by predicting levels of TVB-N and acid value in fish	F	MoX sensor	Regression	SVM, RF	[191]
Detect indoor air contaminants such as CO and CO_2 in the presence of temperature variations	E	MoX sensor	Classification and Regression	SVM SVR, ANN, ELM	[192]
Detect CO, LPG, smoke and CO_2 for early detection of gas leakage and fires	E	MoX sensor	Classification	LR, kNN, NB, CART, SVM, LDA	[193]
Determine the presence of COPD by detecting iso-butane, ammonia, ethanol, carbon monoxide	H	MoX sensor	Classification	SVM, PCA	[194]
Identify the presence of kidney disease by testing for ammonia concentrations	H	Polyaniline nanocomposite sensor	Classification	LDA, RF, SVM, MLP	[195]
Detect odor from cyanobacteria in water reservoirs to mitigate water pollution	E	MoX sensor	Classification	PCA, MLP, LVQ	[196]
Detect the amount of milk rancidity by detecting presence of acetone, toluene, heptanal, limonene and other VOCs	F	MoX sensor	Classification	PCA	[197]
Assess the peach quality index interim of sugar content and acidity using pH level	F	MoX sensor	Regression	PCR, PLS	[198]
Monitor and assess the quality of paddy using biomarkers such as hexanal, heptanal, octanal, ammonia and other VOCs	F	MoX sensor	Regression	MLR	[199]
Classify and discriminate of gas mixtures and assess the concentration of gases present	E	Mixed-potential electrochemical sensors	Classification and Regression	Kernel-based SVM	[200, 201]

Note: E-Environment Management, H-Health Management, F-Food Quality Control

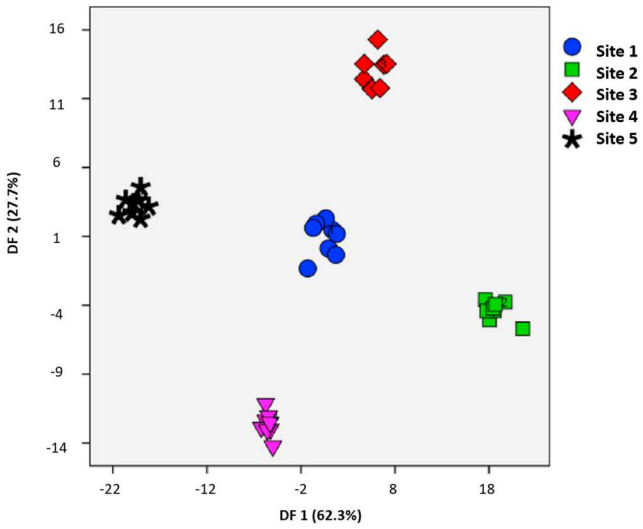

Fig. 23. Results of DFA for the classification of different gases at five different sites. Reproduced with permission from [205].

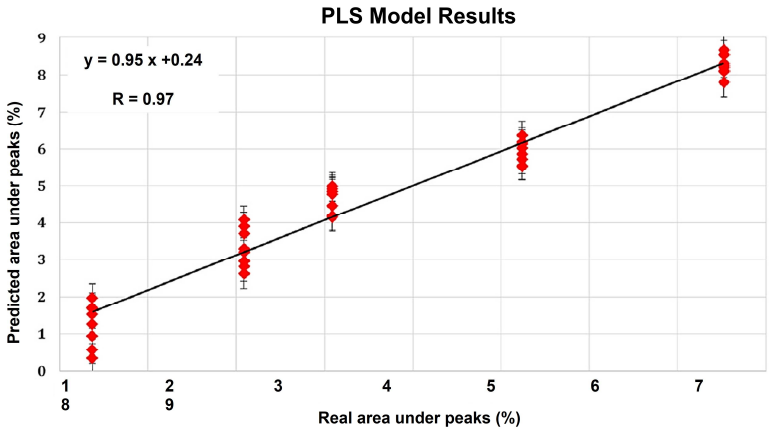

Fig. 24. PLS regression for estimating concentration of the eight VOCs. Reproduced with permission from [205].

In terms of machine learning, exposure to ammonia warranted the need for identifying and quantifying ammonia concentrations in order to undertake mitigation measures. As a consequence, Lei et al. [207] implemented a BPNN model with nine hidden layers and two output layers for the quantitative prediction of the known ammonia concentrations with a 100% prediction rate. Besides ammonia, a linear regression model was proposed by Kumar et al. [212] for predicting levels of ammonia, carbon monoxide, acetone and carbon dioxide in the Indian region of New Delhi, India. The results indicated the effectiveness of the linear regression model but also highlighted the need to incorporate factors like traffic density and unprecedented weather changes to get more accurate results. A similar two-tier approach using the SVM model was discussed by Pace et al. [213] for the detection of hazardous gases in an oil refinery, located in Baghdad, Iraq. The approach used five sensors of different types including MoX, catalytic, and electrochemical to detect the presence of methane, pentane, oxygen, hydrogen sulfide and hexane. An SVM kernel-based model was successfully trained and tested to classify the five different VOCs. Subsequently, the linear regression model built to estimate the gas concentrations yielded low estimation errors, hence, fortifying the potential of both the SVM and the linear regression model.

Detecting toxic hazardous gases can also be beneficial for mitigating accidents in mines as suggested by Nath et al. [214]. Production of methane gas in underground mines can result in the small fires, generating hazardous gases like NO_2 and CO. To expand further on the use of existing sensors, Nath et al. [214] have proposed an IoT-based sensor framework for the fast and reliable detection of toxic gases at mines. The framework utilizes four Au-based MoX gas sensors (TiO_2, CuO, ZnO and WO_3) with high selectivity and sensitivity for detecting the gas concentration inside the mine. The real-time data obtained from the sensors is sent to the microprocessor inside the main control unit and stored in the cloud server. Once collected, the readings in the sensor data are compared to the respective gas thresholds, to take any mitigation measures whenever needed. The results reported in [214] demonstrated the superior performance of gas sensors when coupled with the IoT framework for detecting poisonous gases at mining locations.

4.2 Health management

Recent advancements in technology have expedited ways in which health can be monitored. Health management includes the detection, prognosis and diagnosis of diseases, which has become increasingly tangible now, given the availability of data. Chronic diseases, such as pulmonary diseases [215], diabetes [216], and cancer [217], have become primary culprits of reduction in life expectancies. As a consequence, this warrants their early detection and diagnosis, efforts for which are now continuously being made using sensor technologies. MoX sensors have started to capitalize on the concept of breath analysis for the detection of a number of diseases. The presence of volatile organic compounds such as formaldehyde, isoprene and acetone in human breath have become crucial biomarkers for several respiratory [218] and cancer [219] related diseases. Owing to these sensors, the popularity of E-noses in this sector has been attributed to their non-invasive approach towards disease detection and diagnosis [220].

Recognizing the ability of E-nose systems, Li et al. [221] designed an E-nose system using 10 MoX sensors to study the ability of the sensors in detecting lung cancer using breath-prints. Data for the study included 268 breath samples, out of which 153 samples were obtained from cancer-free individuals, and 115 samples from patients who were pre-diagnosed with lung cancer. Once the samples were acquired, the data was subjected to signal pre-processing for baseline manipulation and noise reduction, followed by data normalization to compensate for the different scale ranges of different sensors. To avoid overfitting of the machine learning model, the study implemented and compared five data dimensionality techniques: PCA, LDA, ICA, k-best features (KBest), and non-negative matrix factorization (NMF). A large overlap between all features was observed using NMF, PCA, KBest and ICA, and as a result, Wang et al. [180] combined the extracted features from LDA with the remaining four techniques to gain a better visualization of data clustering (See Fig. 25). In doing so, the selected features demonstrated a good capability of discriminating between the two classes of individuals which was further observed in the classification accuracy obtained using 3-fold cross validation for RF which reached *86.42%*.

In addition to the exclusive use of MoX sensors, Chen et al. [222] deployed 14 gas sensors of different types including MoX, hot-wire, catalytic and electrochemical gas sensors in an effort to improve the diagnostic capabilities of the E-nose. 235 breath samples were collected from both healthy individuals and patients who conceived lung cancer to study the detection performance of machine leaning algorithms. Following the signal pre-processing which comprised baseline manipulation, noise filtering, and normalization, the authors implemented the kernel PCA (kPCA) to extract relevant features from the sensor response to aid in classification. Through 10-fold leave one out cross validation, Chen et al. [223] randomly segregated the dataset into ten subsets to implement the SVM and XGBoost classification models. The results of the classification favored the combination of kPCA and XGBoost for the detection and staging of lung cancer, with accuracies of *93.59%* and *82.42%* respectively. As an additional step, the models also classified patients with lung cancer or chronic obstructive pulmonary disease (COPD) (highest accuracy of *96%* when applying kPCA-XGBoost) and patients with lung cancer or high-risk of lung cancer (highest accuracy of *93.33%* when using PCA-XGBoost).

Besides lung cancer, cardiovascular diseases have also been at the forefront for rising mortality rates. Earlier, the possibility of a heart disease was studied using patient data such as age, cholesterol and blood sugar levels [223]. However, the cost-effective and non-invasive approach of E-noses has garnered immense attention for the early diagnosis of heart and respiratory diseases. This has been corroborated by the presence of several VOCs in exhaled breath (ethanol, toluene, isobutane) which can serve as potential biomarkers for detecting heart-related issues. Tozlu et al. [224] demonstrated the capability of E-noses for detecting myocardial infraction (MI) using 18 MoX sensors and one moisture sensor for extracting breath samples from healthy individuals, patients with MI, and patients with stable coronary artery disease (SCAD). Their experimental set-up is shown in Fig. 26, wherein 362 breath samples were collected from 33 patients with MI, 22 patients with SCAD and 26 healthy individuals.

The main features including the mean, skewness, kurtosis and variance of the derivative were extracted from the sensor signals to test classification models such as the kNN, SVM and the ANN. To achieve good prediction levels, the wrapper technique of SFE was implemented to determine the most optimal feature set for the 2-step classification. The classification was demarcated into two steps to gain better insight on the models' performance and was reiterated 100 times to achieve model robustness. As a result, classification between MI patients and other individuals rendered an accuracy of *94.1%* using SVM with the most robust classification performance, whereas classification between SCAD patients and healthy individuals was found to be *85%* using the ANN model. Moreover, chronic kidney disease (CKD) is also considered to be a severe complication of cardiovascular diseases and diabetes [225]. The early diagnosis of this health problem can help to expedite viable treatment options. Using three thick-film based MoX sensors, Voss et al. [226] were able to capitalize on their high sensitivity to measure body odor of 42 patients with end renal failure, 20 patients with chronic renal failure and 11 healthy individuals. Using PC1 and PC2 from PCA, Quadrant Discriminant Analysis yielded a classification accuracy of *95.2%* for patients with renal failure, and an accuracy of *98.4%* using PC1 and PC3.

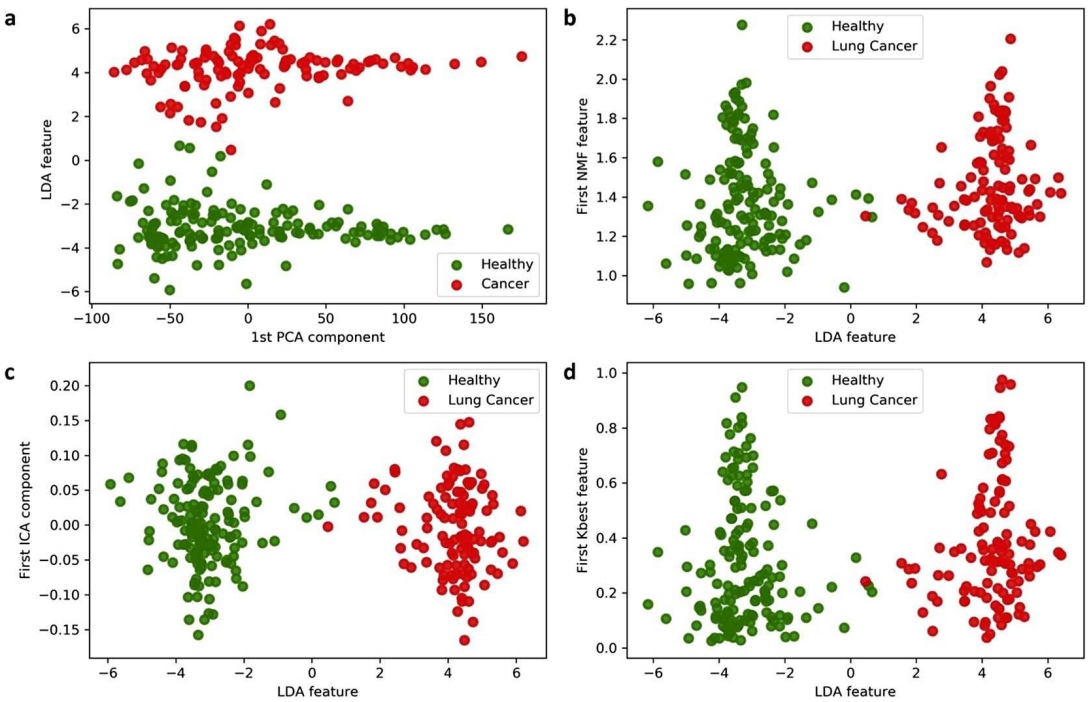

Fig. 25. Data mapping of breath sample features by combining LDA with a) PCA, b) NMF, c) ICA, d) KBest. Reproduced with permission from [221].

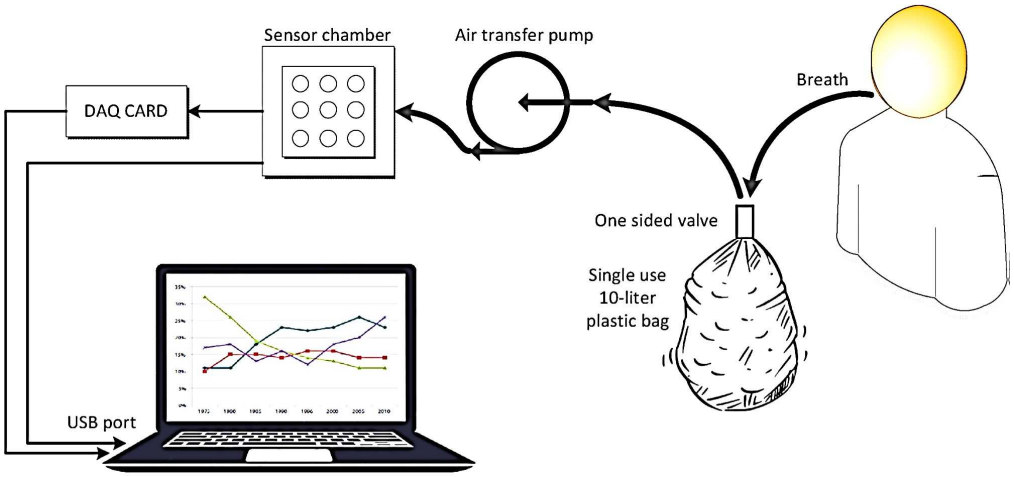

Fig. 26. Block diagram of data acquisition system. Breath samples are collected from individuals in a 10L sample bag and then transferred to the sensor chamber. DAQ is used for the digital conversion of the data for further observations. Reproduced with permission from [224].

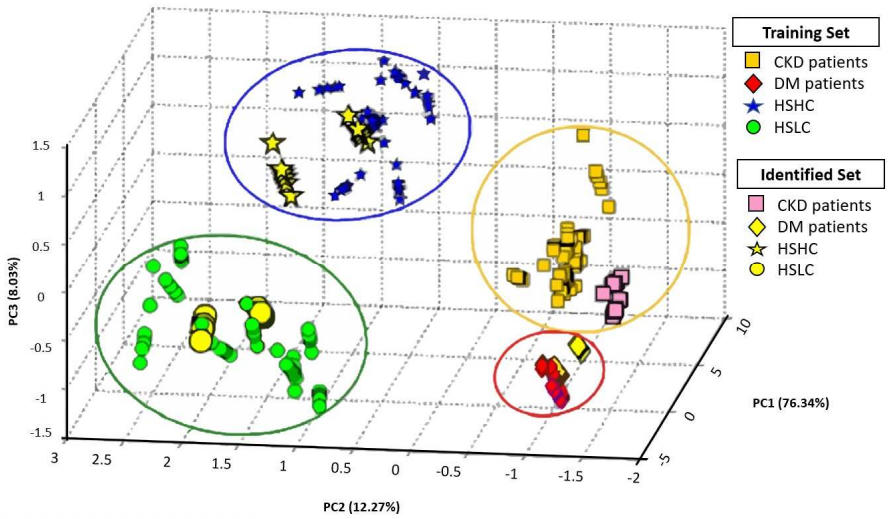

Fig. 27. Projection of dataset using three PCs for the training set and the identified set. Reproduced with permission from [227].

To further highlight the significance of the early identification of CKD and diabetes, Saidi et al. [227] proposed the use of six SnO_2 plated sensors to collect a total of 264 breath samples to distinguish between patients with CKD, diabetes mellitus (DM), patients with high creatinine (HC) and patients with low creatinine (LC). The authors extracted three features from the sensor signals: slope of the conductance, area under the curve and change in conductance between the initial and the exposure phase, thereby rendering a complete feature set with 18 input features. The results from PCA, displayed in Fig. 27, reveal a clear separation between the four classes for the training dataset. In addition, on testing with new samples (Identified set), the results of the PCA model still hold, fortifying its classification performance. Finally, the classification using the SVM model further reinforced the results obtained using PCA, rendering an accuracy of *100%* for discriminating the four different classes.

In putting to use the diagnostic ability of E-noses, Benedek et al. [228] investigated the E-nose operation in detecting sleep apnoea among children. This was observed to be a common disorder among children with an occurrence possibility of 1-3% and limited investigative studies. Benedek et al. [228] aimed to compare breath samples from children for differentiating between obstructive sleep apnoea syndrome (OSAS) and habitual snorers. Using polysomnography, the breathing irregularities were rated based on the apnoea hypopnea index (AHI) as mild (AHI=1), moderate (AHI 6-10), and severe (AHI>10), following which the breath samples from 18 children with OSAS and 10 healthy children were collected using 32 carbon-black polymer sensors. When using PCA technique, PC3 was capable of discriminating between children who had OSAS and those who were habitual snorers with a cross-validation accuracy of *64%*. The results of the PCs were also implemented on a logistic regression model which rendered a sensitivity and specificity of *78%* and *70%*, respectively and with *75%* classification accuracy.

Early detection of pneumonia amongst patients admitted in the ICU was proposed by Liao et al. [229] on observing rising infection rates in the absence of rapid screening procedures. Intubation and mechanical ventilation are considered as major causes of "hospital-acquired pneumonia", rendering high rates of bacterial infections. Although gas chromatography-mass spectrometry helps to identify the presence of pneumonia using VOCs, its time-consuming process makes it infeasible for rapid detection. As a result, Liao et al. [229] suggested the installation of an E-nose within the ventilator system for the early-state detection of pneumonia. The E-nose system was composed of 28 MoX sensors made of SnO_2 and ZnO_2 to detect the presence of the *Pseudomonas aeruginosa* bacteria. The analysis was carried out using 40 patients (20 pneumonia patients and 20 healthy patients) by acquiring 120 samples per patient for a total of 4800 sample data points. For classification, the authors employed a radial basis polynomial kernel (RBPK) function based SVM technique and the ANN approach using a sigmoid activation function. Following a 5-fold cross validation, SVM rendered an accuracy of *92.08%* as opposed to an accuracy of *85.47%* using ANN, thus, demonstrating the ability of an in-built E-nose system to accurately predict early stages of pneumonia.

Gases such as H_2S, NH_3 and CO_2 arising from sites with gas leakage can be potentially adverse for human health. Given the characteristics of MoX sensors, wherein, these sensors suffer from high power consumption rates and low specificity, Kanaparthi and Singh [230] introduced a novel method by using a single ZnO gas sensor. Using a technique referred to as "temperature sweeping" with a "ternary logic", Kanaparthi and Singh [230] recorded the response of the sensor at different temperatures, resulting in 522 features to be further used for classification using Naïve Bayes (NB), SVM, RF and Linear Regression (LR). The dataset was divided into the training and testing datasets in the 80:20 ratio. Using only the responses of the sensor to the three gases, the highest attained accuracy was *85%* using LR. On the other hand, capitalizing on the ternary logic proposed by Kanaparthi and Singh [230], the accuracy increased to *99.8%* using RF. Consequently, the results of this work demonstrated the possibility of using a single MoX gas sensor to simultaneously detect multiple gases, which would otherwise prove detrimental to human health.

4.3 Food quality control

Efforts for evaluating the quality of food have advanced considerably given the safety and health regulations that form an integral part of the food industry. Replacing conventional techniques has become relatively easier since the advent of E-nose, which provides a non-destructive approach to assessing food quality [231]. To benefit from odor samples that can help in rapid food assessments, Wojnowski et al. [232] used electrochemical sensors to detect CO, ethanol H_2S, NO_2, SO_2, and other VOCs for analysis of 75 poultry meat samples and 50 vegetable oil samples. The regular approach for analyzing poultry meat requires studying the total volatile base nitrogen (TVB-N) and the total bacterial count (TBC). A few research studies have been conducted on the use of electrochemical sensors for food quality control. Wojnowski et al. [231] implemented PCA on the sensor signals to identify the principal components for use in the classification of meat samples. When using 66% of the data for training, PC1 and PC2, the SVM classifier provided an accuracy of *98.7%*. On the other hand, thermal degradation of vegetable oils was assessed using the first three principal components followed by an SVM classifier with a staggering accuracy of *100%*. In addition, the research in [232], also reported an analysis for the detection of adulterants in vegetable oils, which include sunflower oil and poor-quality olive oil. The results from SVM with the radial basis function (RBF) kernel reached *82.4%* accuracy with minor misclassifications.

Besides poultry testing, researchers have also explored the use of E-nose systems for monitoring the quality of beef [233, 234]. In a recent study, Wijaya et al. [235] used MoX sensors to study protein and carbohydrate degradation in 12 beef samples through VOCs such CO_2, H_2S, ammonia, methane, aldehydes and ketone. Owing to the high sensitivity of these sensors, 2,220 measurement points were acquired for each beef sample, resulting in a massive dataset of 26,640 measurement points. Wijaya et al. [235] designed a discrete wavelet transform long short-term memory (DWTLSTM) model to classify the quality of the beef samples into three categories: excellent, good, acceptable and spoiled, and estimate the total viable count (TVC) within the beef sample. A comparison of various classification techniques yielded the highest classification accuracies from the long short-term memory (LSTM) (*85.14%*) and DWTLSTM (*94.83%*) models. Although these models gave the best classification accuracies, models like SVM with an accuracy of *84.88%* also fared well. In light of predicting the concentration of bacteria within the beef sample, a comparison of the R^2 and mean squared error (*MSE*), showed that the DWTLSTM model achieves the best performance with an R^2 value of *0.9712* and an MSE of *0.0515*. On closer inspection, kNN, LDA and SVR performed better than multilayer perceptron (MLP) in terms of higher R^2 values and a lower MSE.

Besides electrochemical sensors, Qui and Wang [236] used 10 MoX sensors to determine the amount of food additives in citrus juices. The sensors were used to detect the presence of benzoic acid and chitosan, different concentrations of which had been previously added to the citrus juices in the study. With 5 different concentrations of both benzoic acid and chitosan, a total of 120 samples were used to perform the regression. The LDA technique aided in dimensionality reduction and visualizing the different samples as shown in Fig. 28. For both additives, LD1 and LD2 provide the highest variance between different classes and lowest variance within the classes. Although same samples for benzoic acid were misclassified, concentrations of 0.0g/kg and 2.0g/kg are well-separated. This shows that the sensor signals can easily distinguish between the different concentration samples. For predicting the additive content concentration of benzoic acid, extreme learning machine (ELM) with R^2 of *0.9105* and RF with R^2 of *0.9141* showed great performance with RF surpassing that of ELM. For chitosan concentrations as well, the use of ELM with R^2 of *0.9140* and RF with R^2 of *0.9395* led to good results, with RF providing the best performance for the detection of both benzoic acid and chitosan concentrations.

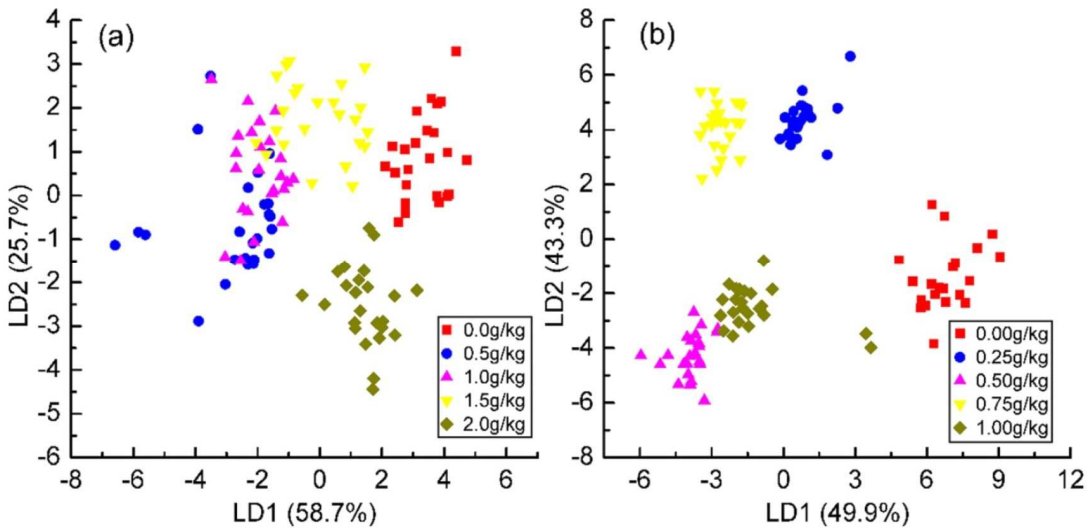

Fig. 28. LDA for citrus juices with a) benzoic acid, b) chitosan. Reproduced with permission from [236].

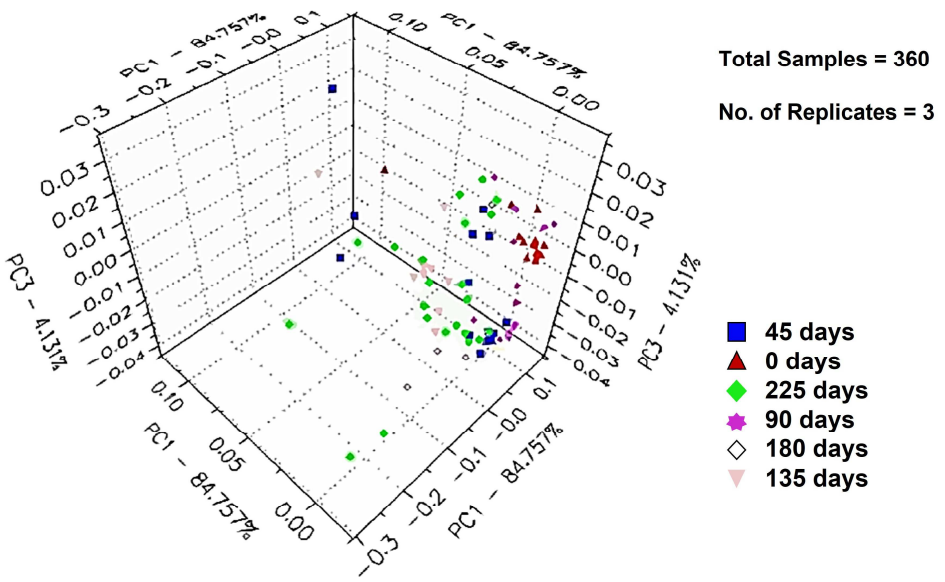

Fig. 29. PCA for rice samples stored over 225 days and fresh rice samples (red triangle). Reproduced with permission from [237].

In an attempt to focus on insect infestation detection, Srivastava et al. [237] designed a fuzzy controller E-nose system to identify the presence of *Sitophilus oryzae* infestation in rice grains. As a staple food-source for many, the use of E-nose for rice infestation detection was undertaken to overcome the challenges presented by traditional methods of sieving and insect trapping. These exorbitant techniques were known to be successful only after the insects have propagated [238], and consequently, the use of volatile biomarkers for their early detection have gained traction. For the experiment, clean rice was used for control samples, whereas infested rice with varying number of insects was kept under observation for further analysis of insect infestation. An E-nose with 18 MoX sensors recorded the sensor responses of volatiles such as aldehydes, ketones, ammonia and uric acid that emanated from the rice aroma and were produced by the insects. With a total of 360 samples, tested over intervals of 45 days, PCA analysis showed a clear distinction between fresh rice samples and rice samples that were stored and tested in interval of 45 days (See Fig. 29). As the days progressed, changes in the uric acid content and a degradation in the protein content were observed. The regression results using multiple linear regression provided predicted content values of protein and uric acid that were in accordance with their measured counterparts. The results proved effective for early infestation detection to adopt grain treatment methods before the infestation is exacerbated.

In addition to the identification of adulteration levels in rice grains, several studies have focused on detecting adulteration in saffron. Saffron, a widely used spice of high quality, has a multitude of benefits such as its medicinal properties as an antidepressant [239] or its physiological impact on patients with diabetes [240]. Traditional methods of analyzing saffron quality have been long forsaken due to their time-consuming and expensive implementation approach. Using the strength of saffron, i.e., its aroma, over the years, E-nose systems have been developed to gauge its quality in an efficient and inexpensive manner. Kiani et al. [241] developed a system that combined computer vision and an E-nose comprised of seven MoX sensors which detected the aroma and color of 33 saffron samples collected from different regions in Iran. PCA results for the authentic samples and 10 adulterated saffron samples indicated *90%* and *5%* variance along PC1 and PC2, respectively. Furthermore, when using 85% of the data for training, authentic saffron samples, and adulterated samples of artificially colored yellow styles of saffron (ACYSS) and artificially colored safflower (ACS) were predicted correctly by SVM with 100% classification accuracy. On the other hand, the ANN-MLP model provided an R^2 of *0.9786* for predicting the level of aroma adulteration, thereby, indicating a good performance of the models for both classification and regression. Prior to this, using only aroma for the quality detection of saffron, Kiani et al. [242] used 10 MoX sensors to detect aroma of 11 saffron samples from Iran. PCA results along the PC1 and PC2 that accounted for 98% of the variance in the data clearly distinguished between the aromas of the 11 saffron samples. The identification of the two sensors that offered the least variance in the data enabled to improve the performance of the ANN-MLP model for classifying the 11 samples into five classes: excellent, very good, good, medium, poor using the remaining 8 sensors. The accuracy increased from *97.5%* to *100%* when using 8 sensors, which fortified the importance of the use of relevant data for achieving good classification results.

5. Summary and Potential Future Work

Gas sensing technology using E-nose systems that combine GSAs and machine learning have witnessed tremendous growth in the recent years. Through various fabrication technologies, different sensors such as MoX, CNT-based, conductive polymer, acoustic, catalytic, optical and MOF-based have been designed to collaborate with machine learning to mimic the human olfactory system. Relying on sensing materials, their ability to detect innumerous gases, followed by the implementation of machine learning algorithms for gas pattern recognition, E-noses have proved to be steadfast in several applications. In areas such as food quality control and health diagnosis where traditional methods of identifying abnormalities through visual examinations are deemed slow and expensive, E-nose systems have attempted to alleviate this challenge. E-nose systems have allowed for the detection of VOCs in a rapid and non-invasive manner to expedite their applications in different fields.

An indispensable part of the E- nose system operation is machine learning itself, and hence, algorithms and software tools widely used for E-nose systems have been discussed in great detail. Among the machine learning approaches, techniques of PCA and LDA have been commonly used for feature extraction to aid in dimensionality reduction. In addition to feature extraction, feature selection for dimensionality reduction has also shown immense potential using both wrapper (SFS, SBE) and filter (gini index, correlation) based techniques. Algorithms such as kNN, SVM, ANN, Decision Tree, Random Forests, and ensemble techniques have been implemented using tools like PyTorch, Weka, Tensorflow and Shogun for various applications. The ensemble techniques demonstrate superior performance with the capability of combining either similar or distinct machine learning models for enhancing the overall performance of the E-nose system.

Despite their unwavering success in several arenas, there are several challenges that persistently hover over E-nose systems and are continuously being addressed to improve their performance. Sensor selectivity and sensitivity still pose a challenge to the GSAs within the E-nose system. This inability to precisely detect the target gas of interest greatly affects the processes of feature extraction and feature selection that follow the sensors' data acquisition. Although researchers have employed ANNs to improve the capability of sensors in this regard [243, 244], significant progress is yet to be achieved to counteract this challenge. In addition, challenges associated to drift have also been addressed by models inspired from PCA [245] and Particle Swarm Optimization [246], wherein, these techniques provide a solution for the short-term compensation of drift. As a consequence, their long-term compensation and alleviation warrants additional research for the development of better sensing materials and machine learning techniques. Moreover, research indicates that the most commonly used sensors for E-nose applications fall under the category of MoX [23] and conductive polymer sensors [27]. Hence, increasing the effectiveness of other sensors requires a greater focus on fabrication technologies to improve their stability and durability, in order to yield better performance in an E-nose system. This might result in larger GSAs for detecting multiple volatiles, however, the challenge of using minimal sensors within an E-nose system for several applications still remains.

Recent studies have introduced the combined use of an E-nose and an E-tongue for assimilating maximum information with minimal cost and higher effectiveness [175]. An electronic tongue also referred to as E-tongue was designed to mimic the taste buds of the human tongue for taste assessments [247]. E-tongues have been used to detect the presence of organic and inorganic compounds, albeit, in aqueous solutions [248, 249]. As discussed in [249], using electrodes dipped in test solutions, the electrode-solution interaction results in varying current, resistance or potential that is subsequently measured by the E-tongue to determine different tastes. The combination of E-tongue and E-nose has recently been adopted in the area of food and beverage [152, 168, 250], and has yielded extremely powerful classification performances in comparison to the performance that would result from an individual E-nose or E-tongue. Despite a high-hold on their good performance, such a combination of sensors demands a large dataset to ensure good repeatability and signal processing in order to obtain a superior performance. This can be achieved by using the optimal combination of sensors, in addition to utilizing appropriate feature extraction techniques. Furthermore, E-nose applications thus far have primarily focused on data that was collected at a particular point in time. Especially for medical applications, continuous monitoring of real-time data using previously trained E-nose systems can help to expedite the diagnostic process and predict severe diseases at early stages. Building further on the work related to E-nose systems, another aspect that could be delved into, is the amalgamation of classification and regression into a single model. The classification of the gas type and the estimation of its concentration have been so far achieved using two separate single-output models. By identifying the best machine learning models, a multiple-output model can be developed that can identify the gas type as well as its concentration simultaneously.

Author Contributions

L. Mahmood conducted research on the various types of gas sensors, on their applications in the real-world, on machine learning approaches and how they can be capitalized on for gas sensing applications. M. Ghommem sat the groundwork for the overall manuscript in terms of the subject and highlighted the critical points of interest within gas sensing technologies. Z. Bahroun initiated the project and provided guidance on the different machine learning techniques discussed in the paper. The manuscript was written through the collaboration and contribution of all the authors. All authors discussed the content, reviewed, and approved the final version of the manuscript.

Acknowledgments

Not applicable.

Conflict of Interest

The authors declared no potential conflicts of interest concerning the research, authorship, and publication of this article.

Funding

M. Ghommem gratefully acknowledges the financial support from American University of Sharjah (grant number FRG21-M-E86) and Sharjah Research Academy (grant number SRA20-023).

Data Availability Statements

The datasets generated and/or analyzed during the current study are available from the corresponding author on reasonable request.

References

[1] Chen, J., Gu, J., Zhang, R., Mao, Y., Tian, S., Freshness Evaluation of Three Kinds of Meats Based on the Electronic Nose, *Sensors (Switzerland)*, 19(3), 2019, 605.

[2] Matindoust, S., Baghaei-Nejad, M., Abadi, M. H. S., Zou, Z., Zheng, L. R., Food Quality and Safety Monitoring Using Gas Sensor Array in Intelligent Packaging, *Sensor Review*, 36(2), 2016, 169–183.

[3] Blanco-Novoa, O., Fernández-Caramés, T. M., Fraga-Lamas, P., Castedo, L., A Cost-Effective IoT System for Monitoring Indoor Radon Gas Concentration, *Sensors (Switzerland)*, 18(7), 2018, 2198.

[4] He, J., Xu, L., Wang, P., Wang, Q., A High Precise E-Nose for Daily Indoor Air Quality Monitoring in Living Environment, *Integration, the VLSI Journal*, 58, 2017, 286–294.

[5] Oosthuizen, D. N., Motaung, D. E., Swart, H. C., Selective Detection of CO at Room Temperature with CuO Nanoplatelets Sensor for Indoor Air Quality Monitoring Manifested by Crystallinity, *Applied Surface Science*, 466, 2019, 545–553.

[6] Kao, K.-W. A., Cheng, C.-J., Gwo, S., Yeh, J. A., A Semiconductor Gas System of Healthcare for Liver Disease Detection Using Ultrathin InN-Based Sensor, *ECS Transactions*, 66(7), 2015, 151–157.

[7] Sonuç Karaboga, M. N., Sezgintürk, M. K., Analysis of Tau-441 Protein in Clinical Samples Using RGO/AuNP Nanocomposite-Supported Disposable Impedimetric Neuro-Biosensing Platform: Towards Alzheimer's Disease Detection, *Talanta*, 219, 2020, 121257.

[8] Guo, K., Yang, P., Guo, D. H., Liu, Y., Gas Leakage Monitoring with Mobile Wireless Sensor Networks, *Procedia Computer Science*, 154, 2018, 430–438.

[9] Joshila Grace, L. K., Sai Teja, K., Sai Kishan Reddy, J. V., A Robotic Platform to Identify Gas Pipe Leakage Using IOT, *IOP Conference Series: Materials Science and Engineering*, 590(1), 2019, 012048.

[10] Ashari, I. A., Widodo, A. P., Suryono, S., The Monitoring System for Ammonia Gas (NH3) Hazard Detection in the Livestock Environment Uses Inverse Distance Weight Method, *Proceedings of 2019 4th International Conference on Informatics and Computing, ICIC 2019*, 2019.

[11] Hunter, G. W. *et al.*, Editors' Choice—Critical Review—A Critical Review of Solid State Gas Sensors, *Journal of the Electrochemical Society*, 167(3), 2020, 037570.

[12] Dey, A., Semiconductor Metal Oxide Gas Sensors: A Review, *Materials Science and Engineering B: Solid-State Materials for Advanced Technology*, 229, 2018, 206–217.

[13] Chen, Z., Chen, Z., Song, Z., Ye, W., Fan, Z., Smart Gas Sensor Arrays Powered by Artificial Intelligence, *Journal of Semiconductors*, 40(11), 2019, 111601.

[14] Feng, S. *et al.*, Review on Smart Gas Sensing Technology, *Sensors (Switzerland)*, 19(17), 2019, 3760.

[15] Gradišek, A. *et al.*, Improving the Chemical Selectivity of an Electronic Nose to TNT, DNT and RDX Using Machine Learning, *Sensors (Switzerland)*, 19(23), 2019, 5207.

[16] Jasinski, G., Influence of Operation Temperature Instability on Gas Sensor Performance, *European Microelectronics Packaging Conference*, Warsaw, Poland, 2017.

[17] Song, R. *et al.*, High Selective Gas Sensors Based on Surface Modified Polymer Transistor, *Organic Electronics*, 91, 2021, 106083.

[18] Fonollosa, J., Fernández, L., Gutiérrez-Gálvez, A., Huerta, R., Marco, S., Calibration Transfer and Drift Counteraction in Chemical Sensor Arrays Using Direct Standardization, *Sensors and Actuators, B: Chemical*, 236, 2016, 1044–1053.

[19] Jafri, R. I., Ramaprabhu, S., Multi Walled Carbon Nanotubes Based Micro Direct Ethanol Fuel Cell Using Printed Circuit Board Technology, *International Journal of Hydrogen Energy*, 35(3), 2010, 1339–1346.

[20] Ruhland, B., Becker, T., Müller, G., Gas-Kinetic Interactions of Nitrous Oxides with SnO2 Surfaces, *Sensors and Actuators B: Chemical*, 50(1), 1998, 85–94.

[21] Vergara, A., Vembu, S., Ayhan, T., Ryan, M. A., Homer, M. L., Huerta, R., Chemical Gas Sensor Drift Compensation Using Classifier Ensembles, *Sensors and Actuators, B: Chemical*, 166–167, 2012, 320–329.

[22] Mielle, P., Managing Dynamic Thermal Exchanges in Commercial Semiconducting Gas Sensors, *Sensors and Actuators B: Chemical*, 34, 1996, 533–538.

[23] Pashami, S., Lilienthal, A. J., Trincavelli, M., Detecting Changes of a Distant Gas Source with an Array of MOX Gas Sensors, *Sensors (Switzerland)*, 12(12), 2012, 16404–16419.

[24] Gomri, S., Contaret, T., Seguin, J. L., A New Gases Identifying Method with MOX Gas Sensors Using Noise Spectroscopy, *IEEE Sensors Journal*, 18(16), 2018, 6489–6496.

[25] Hübner, M., Simion, C. E., Tomescu-Stanoiu, A., Pokhrel, S., Bârsan, N., Weimar, U., Influence of Humidity on CO Sensing with P-Type CuO Thick Film Gas Sensors, *Sensors and Actuators, B: Chemical*, 153(2), 2011, 347–353.

[26] Wu, Y., Yuan, L., Hua, Z., Zhen, D., Qiu, Z., Design and Optimization of Heating Plate for Metal Oxide Semiconductor Gas Sensor, *Microsystem Technologies*, 25(9), 2019, 3511–3519.

[27] Park, C. S., Kim, D. H., Shin, B. J., Kim, D. Y., Lee, H. K., Tae, H. S., Conductive Polymer Synthesis with Single-Crystallinity via a Novel Plasma Polymerization Technique for Gas Sensor Applications, *Materials*, 9(10), 2016, 812.

[28] Esteves, C. H. A., Iglesias, B. A., Li, R. W. C., Ogawa, T., Araki, K., Gruber, J., New Composite Porphyrin-Conductive Polymer Gas Sensors for Application in Electronic Noses, *Sensors and Actuators, B: Chemical*, 193, 2014, 136–141.

[29] Dube, I. *et al.*, Understanding the Electrical Response and Sensing Mechanism of Carbon-Nanotube-Based Gas Sensors, *Carbon*, 87(C), 2015, 330–337.

[30] Ueda, T., Bhuiyan, M. M. H., Norimatsu, H., Katsuki, S., Ikegami, T., Mitsugi, F., Development of Carbon Nanotube-Based Gas Sensors for NOx Gas Detection Working at Low Temperature, *Physica E: Low-Dimensional Systems and Nanostructures*, 40(7), 2008, 2272–2277.

[31] Sayago, I. *et al.*, New Sensitive Layers for Surface Acoustic Wave Gas Sensors Based on Polymer and Carbon Nanotube Composites, *Sensors and Actuators, B: Chemical*, 175, 2012, 67–72.

[32] van Quy, N., Minh, V. A., van Luan, N., Hung, V. N., van Hieu, N., Gas Sensing Properties at Room Temperature of a Quartz Crystal Microbalance Coated with ZnO Nanorods, *Sensors and Actuators, B: Chemical*, 153(1), 2011, 188–193.

[33] Xu, L., Li, T., Gao, X., Wang, Y., A High Heating Efficiency Two-Beam Microhotplate for Catalytic Gas Sensors, *2012 7th IEEE International Conference on Nano/Micro Engineered and Molecular Systems, NEMS 2012*, 65–68, 2012.

[34] Xu, L., Wang, Y., Zhou, H., Liu, Y., Li, T., Wang, Y., Design, Fabrication, and Characterization of a High-Heating-Efficiency 3-D Microheater for Catalytic Gas Sensors, *Journal of Microelectromechanical Systems*, 21(6), 2012, 1402–1409.

[35] Wang, L., Metal-Organic Frameworks for QCM-Based Gas Sensors: A Review, *Sensors and Actuators, A: Physical*, 307, 2020, 111984.

[36] Drobek, M., Kim, J. H., Bechelany, M., Vallicari, C., Julbe, A., Kim, S. S., MOF-Based Membrane Encapsulated ZnO Nanowires for Enhanced Gas Sensor Selectivity, *ACS Applied Materials and Interfaces*, 8(13), 2016, 8323–8328.

[37] Pohle, R., Tawil, A., Davydovskaya, P., Fleischer, M., Metal Organic Frameworks as Promising High Surface Area Material for Work Function Gas Sensors, *Procedia Engineering*, 25, 2011, 108–111.

[38] Lochbaum, A., Fedoryshyn, Y., Dorodnyy, A., Koch, U., Hafner, C., Leuthold, J., On-Chip Narrowband Thermal Emitter for Mid-IR Optical Gas Sensing, *ACS Photonics*, 4(6), 2017, 1371–1380.

[39] Paliwal, A., Sharma, A., Tomar, M., Gupta, V., Carbon Monoxide (CO) Optical Gas Sensor Based on ZnO Thin Films, *Sensors and Actuators, B: Chemical*, 250, 2017, 679–685.

[40] Kornienko, V. v. *et al.*, Machine Learning for Optical Gas Sensing: A Leaky-Mode Humidity Sensor as Example, *IEEE Sensors Journal*, 20(13), 2020, 6954–6963.

[41] Bhopate, D. *et al.*, Fluorescent Chemosensor for Quantitation of Multiple Atmospheric Gases, *Journal of Nanomedicine & Nanotechnology*, 8(2), 2017, 1000436.

[42] Liu, Y. H., Chang, S. J., Lai, L. T., Tu, Y. P., Young, S. J., Aluminum-Doped Zinc Oxide Nanorods and Methyl Alcohol Gas Sensor Application, *Microsystem Technologies*, 28, 2022, 377–382.

[43] Choi, K. J., Jang, H. W., One-Dimensional Oxide Nanostructures as Gas-Sensing Materials: Review and Issues, *Sensors*, 10(4), 2010, 4083–4099.

[44] Degler, D., Weimar, U., Barsan, N., Current Understanding of the Fundamental Mechanisms of Doped and Loaded Semiconducting Metal-Oxide-Based Gas Sensing Materials, *ACS Sensors*, 4(9), 2019, 2228–2249.

[45] Collier-Oxandale, A. M., Thorson, J., Halliday, H., Milford, J., Hannigan, M., Understanding the Ability of Low-Cost MOx Sensors to Quantify Ambient VOCs, *Atmospheric Measurement Techniques*, 12(3), 2019, 1441–1460.

[46] Ciciotti, F., Baschirotto, A., Buffa, C., Gaggl, R., A MOX Gas Sensors Resistance-to-Digital CMOS Interface with 8-Bits Resolution and 128dB Dynamic Range for Low-Power Consumer Applications, *PRIME 2017 - 13th Conference on PhD Research in Microelectronics and Electronics, Proceedings*, 21–24, 2017.

[47] Albert, K. J. *et al.*, Cross-Reactive Chemical Sensor Arrays, *Chemical Reviews*, 100(7), 2000, 2595–2626.

[48] Martinez, D., Burgués, J., Marco, S., Fast Measurements with MOX Sensors: A Least-Squares Approach to Blind Deconvolution, *Sensors (Switzerland)*, 19(18), 2019, 4029.

[49] Rebholz, J. *et al.*, Selectivity Enhancement by Using Double-Layer Mox-Based Gas Sensors Prepared by Flame Spray Pyrolysis (FSP), *Sensors (Switzerland)*, 16(9), 2016, 1437.

[50] Bierer, B., Kneer, J., Wöllenstein, J., Palzer, S., MEMS Based Metal Oxide Sensor for Simultaneous Measurement of Gas Induced Changes of the Heating Power and the Sensing Resistance, *Microsystem Technologies*, 22(7), 2016, 1855–1863.

[51] Palzer, S., Moretton, E., Ramirez, F. H., Romano-Rodriguez, A., Wöllenstein, J., Nano- and Microsized Metal Oxide Thin Film Gas Sensors, *Microsystem Technologies*, 14(4–5), 2008, 645–651.

[52] Faglia, G. *et al.*, Micromachined Gas Sensors for Environmental Pollutants, *Microsystem Technologies*, 6(2), 1999, 54–59.

[53] Gessner, T. *et al.*, Metal Oxide Gas Sensor for High Temperature Application, *Microsystem Technologies*, 6, 2000, 169–174.

[54] Prajesh, R., Goyal, V., Saini, V., Bhargava, J., Sharma, A., Agarwal, A., Development and Reliability Analysis of Micro Gas Sensor Platform on Glass Substrate, *Microsystem Technologies*, 25(9), 2019, 3589–3597.

[55] Nambiar, S., Yeow, J. T. W., Conductive Polymer-Based Sensors for Biomedical Applications, *Biosensors and Bioelectronics*, 26(5), 2011, 1825–1832.
[56] Liu, H. *et al.*, Electrically Conductive Polymer Composites for Smart Flexible Strain Sensors: A Critical Review, *Journal of Materials Chemistry C*, 6(45), 2018, 12121–12141.
[57] Holze, R., Wu, Y. P., Intrinsically Conducting Polymers in Electrochemical Energy Technology: Trends and Progress, *Electrochimica Acta*, 122, 2014, 93–107.
[58] Bai, H., Shi, G., Gas Sensors Based on Conducting Polymers, *Sensors*, 7, 2007, 267–307.
[59] Zamiri, G., Haseeb, A. S. M. A., Recent Trends and Developments in Graphene/Conducting Polymer Nanocomposites Chemiresistive Sensors, *Materials*, 13(15), 2020, 3311.
[60] Pandhi, T., Chandnani, A., Subbaraman, H., Estrada, D., A Review of Inkjet Printed Graphene and Carbon Nanotubes Based Gas Sensors, *Sensors (Switzerland)*, 20(19), 2020, 1–20.
[61] Tang, R., Shi, Y., Hou, Z., Wei, L., Carbon Nanotube-Based Chemiresistive Sensors, *Sensors (Switzerland)*, 17(4), 2017, 882.
[62] Akbari, E. *et al.*, Analytical Calculation of Sensing Parameters on Carbon Nanotube Based Gas Sensors, *Sensors (Switzerland)*, 14(3), 2014, 5502–5515.
[63] Hoang, N. D., van Cat, V., Nam, M. H., Phan, V. N., Le, A. T., van Quy, N., Enhanced SO2 Sensing Characteristics of Multi-Wall Carbon Nanotubes Based Mass-Type Sensor Using Two-Step Purification Process, *Sensors and Actuators, A: Physical*, 295, 2019, 696–702.
[64] Casanova-Cháfer, J., Navarrete, E., Noirfalise, X., Umek, P., Bittencourt, C., Llobet, E., Gas Sensing with Iridium Oxide Nanoparticle Decorated Carbon Nanotubes, *Sensors (Switzerland)*, 19(1), 2019, 113.
[65] Selvakumar, V. S., Sujatha, L., Fast Response and Recovery of Nano-Porous Silicon Based Gas Sensor, *Microsystem Technologies*, 26(3), 2020, 823–834.
[66] Seals, L., Gole, J. L., Tse, L. A., Hesketh, P. J., Rapid, Reversible, Sensitive Porous Silicon Gas Sensor, *Journal of Applied Physics*, 91(4), 2002, 2519–2523.
[67] Baratto, C. *et al.*, A Novel Porous Silicon Sensor for Detection of Sub-Ppm NO2 Concentrations, *Sensors and Actuators, B: Chemical*, 77(1–2), 2001, 62–66.
[68] Sabdo Yuwono, A., Schulze Lammers, P., Odor Pollution in the Environment and the Detection Instrumentation, *Agricultural Engineering International: The CIGR Journal of Scientific Research and Development*, 1, 2004, 552.
[69] Yang, M., He, J., Hu, X., Yan, C., Cheng, Z., CuO Nanostructures as Quartz Crystal Microbalance Sensing Layers for Detection of Trace Hydrogen Cyanide Gas, *Environmental Science and Technology*, 45(14), 2011, 6088–6094.
[70] Alev, O., Sarıca, N., Özdemir, O., Arslan, L. Ç., Büyükköse, S., Öztürk, Z. Z., Cu-Doped ZnO Nanorods Based QCM Sensor for Hazardous Gases, *Journal of Alloys and Compounds*, 826, 2020, 154177.
[71] Liu, X., Wang, W., Zhang, Y., Pan, Y., Liang, Y., Li, J., Enhanced Sensitivity of a Hydrogen Sulfide Sensor Based on Surface Acoustic Waves at Room Temperature, *Sensors (Switzerland)*, 18(11), 2018, 3796.
[72] Mariani, E. A., Mariani, E. A., US Patent No. 5325704, 1994.
[73] Jakubik, W. P., Surface Acoustic Wave-Based Gas Sensors, *Thin Solid Films*, 520(3), 2011, 986–993.
[74] Fan, L., Ge, H., Zhang, S. Y., Zhang, H., Zhu, J., Optimization of Sensitivity Induced by Surface Conductivity and Sorbed Mass in Surface Acoustic Wave Gas Sensors, *Sensors and Actuators, B: Chemical*, 161(1), 2012, 114–123.
[75] Bhasker Raj, V., Singh, H., Nimal, A. T., Tomar, M., Sharma, M. U., Gupta, V., Effect of Metal Oxide Sensing Layers on the Distinct Detection of Ammonia Using Surface Acoustic Wave (SAW) Sensors, *Sensors and Actuators, B: Chemical*, 187, 2013, 563–573.
[76] Lukman Hekiem, N. L. *et al.*, Advanced Vapour Sensing Materials: Existing and Latent to Acoustic Wave Sensors for VOCs Detection as the Potential Exhaled Breath Biomarkers for Lung Cancer, *Sensors and Actuators, A: Physical*, 329, 2021, 112792.
[77] Panneerselvam, G., Thirumal, V., Pandya, H. M., Review of Surface Acoustic Wave Sensors for the Detection and Identification of Toxic Environmental Gases/Vapours, *Archives of Acoustics*, 43(3), 2018, 357–367.
[78] Karelin, A., Baranov, A. M., Akbari, S., Mironov, S., Karpova, E., Measurement Algorithm for Determining Unknown Flammable Gas Concentration Based on Temperature Sensitivity of Catalytic Sensor, *IEEE Sensors Journal*, 19(11), 2019, 4173–4180.
[79] Lee, E. B. *et al.*, Micromachined Catalytic Combustible Hydrogen Gas Sensor, *Sensors and Actuators, B: Chemical*, 153(2), 2011, 392–397.
[80] Brauns, E., Morsbach, E., Kunz, S., Bäumer, M., Lang, W., A Fast and Sensitive Catalytic Gas Sensors for Hydrogen Detection Based on Stabilized Nanoparticles as Catalytic Layer, *Sensors and Actuators, B: Chemical*, 193, 2014, 895–903.
[81] Hu, Y., Tian, Y., Zhuang, Y., Zhao, C., Wang, F., Rapid Gas Sensing Based on Pulse Heating and Deep Learning, *2021 IEEE 34th International Conference on Micro Electro Mechanical Systems (MEMS)*, 2021-January, 438–441, 2021.
[82] Sturm, H., Brauns, E., Seemann, T., Zoellmer, V., Lang, W., A Highly Sensitive Catalytic Gas Sensor for Hydrogen Detection Based on Sputtered Nanoporous Platinum, *Procedia Engineering*, 5, 2010, 123–126.
[83] Jaber, N., Ilyas, S., Shekhah, O., Eddaoudi, M., Younis, M. I., Resonant Gas Sensor and Switch Operating in Air with Metal-Organic Frameworks Coating, *Journal of Microelectromechanical Systems*, 27(2), 2018, 156–163.
[84] Jaber, N., Ilyas, S., Shekhah, O., Eddaoudi, M., Younis, M. I., Multimode Excitation of a Metal Organics Frameworks Coated Microbeam for Smart Gas Sensing and Actuation, *Sensors and Actuators, A: Physical*, 283, 2018, 254–262.
[85] Jaber, N., Ilyas, S., Shekhah, O., Eddaoudi, M., Younis, M. I., Smart Gas Sensing and Actuation Using Multimode of a MOFs Coated Microbeam, *Proceedings of IEEE Sensors*, 2018-October, 2018.
[86] Jaber, N., Ilyas, S., Shekhah, O., Eddaoudi, M., Younis, M. I., Simultaneous Sensing of Vapor Concentration and Temperature Utilizing Multimode of a MEMS Resonator, *Proceedings of IEEE Sensors*, 2018-October, 2018.
[87] Ghommem, M., Puzyrev, V., Sabouni, R., Najar, F., Deep Learning for Gas Sensing Using MOFs Coated Weakly-Coupled Microbeams, *Applied Mathematical Modelling*, 105, 2022, 711-728.
[88] Sepulveda, N., Aslam, D., Sullivan, J. P., Polycrystalline Diamond MEMS Resonator Technology for Sensor Applications, *Diamond and Related Materials*, 15(2–3), 2006, 398–403.
[89] Massie, C., Stewart, G., McGregor, G., Gilchrist, J. R., Design of a Portable Optical Sensor for Methane Gas Detection, *Sensors and Actuators, B: Chemical*, 113(2), 2006, 830–836.
[90] Jin, W., Ho, H. L., Cao, Y. C., Ju, J., Qi, L. F., Gas Detection with Micro- and Nano-Engineered Optical Fibers, *Optical Fiber Technology*, 19(6 PART B), 2013, 741–759.
[91] Garcia-Romeo, D., Fuentes, H., Medrano, N., Calvo, B., Martínez, P. A., Azcona, C., A NDIR-Based CO2 Monitor System for Wireless Sensor Networks, *2012 IEEE 3rd Latin American Symposium on Circuits and Systems, LASCAS 2012 - Conference Proceedings*, 2012.
[92] Tan, Q. *et al.*, Three-Gas Detection System with IR Optical Sensor Based on NDIR Technology, *Optics and Lasers in Engineering*, 74, 2015, 103–108.
[93] Kudo, H. *et al.*, Fiber-Optic Biochemical Gas Sensor (Bio-Sniffer) for Sub-Ppb Monitoring of Formaldehyde Vapor, *Sensors and Actuators, B: Chemical*, 161(1), 2012, 486–492.
[94] Zhu, Y., Shi, J., Zhang, Z., Zhang, C., Zhang, X., Development of a Gas Sensor Utilizing Chemiluminescence on Nanosized Titanium Dioxide, *Analytical Chemistry*, 74(1), 2002, 120–124.
[95] Lv, Y. Y., Wu, J., Xu, Z. K., Colorimetric and Fluorescent Sensor Constructing from the Nanofibrous Membrane of Porphyrinated Polyimide for the Detection of Hydrogen Chloride Gas, *Sensors and Actuators, B: Chemical*, 148(1), 2010, 233–239.
[96] Wang, X. D., Wolfbeis, O. S., Optical Methods for Sensing and Imaging Oxygen: Materials, Spectroscopies and Applications, *Chemical Society Reviews*, 43(10), 2014, 3666–3761.
[97] Vafaei, M., Amini, A., Siadatan, A., Breakthrough in CO2 Measurement with a Chamberless NDIR Optical Gas Sensor, *IEEE Transactions on Instrumentation and Measurement*, 69(5), 2020, 2258–2268.
[98] Zhang, W., Tian, F., Song, A., Hu, Y., Research on Electronic Nose System Based on Continuous Wide Spectral Gas Sensing, *Microchemical Journal*, 140, 2018, 1–7.
[99] Ma, D., Gao, J., Zhang, Z., Zhao, H., Gas Recognition Method Based on the Deep Learning Model of Sensor Array Response Map, *Sensors and Actuators, B: Chemical*, 330, 2021, 129349.
[100] Storcheus, D., Rostamizadeh, A., Kumar, S., The 1st International Workshop "Feature Extraction: Modern Questions and Challenges" A Survey of Modern Questions and Challenges in Feature Extraction Google Research Google Research, 2015.
[101] Patgiri, R., Katari, H., Kumar, R., Sharma, D., Empirical Study on Malicious URL Detection Using Machine Learning, *Lecture Notes in Computer*

Science (including subseries Lecture Notes in Artificial Intelligence and Lecture Notes in Bioinformatics), 11319, 2019, 380–388.
[102] Li, W., Leung, H., Kwan, C., Linnell, B. R., E-Nose Vapor Identification Based on Dempster-Shafer Fusion of Multiple Classifiers, *IEEE Transactions on Instrumentation and Measurement*, 57(10), 2008, 2273–2282.
[103] Khalaf, W., Pace, C., Gaudioso, M., Gas Detection via Machine Learning, *International Journal Electrical and Computer Engineering*, 3(5), 2008, 1–5.
[104] Yu, H., Wang, J., Yao, C., Zhang, H., Yu, Y., Quality Grade Identification of Green Tea Using E-Nose by CA and ANN, *LWT - Food Science and Technology*, 41(7), 2008, 1268–1273.
[105] Li, Q., Gu, Y., Wang, N. F., Application of Random Forest Classifier by Means of a QCM-Based E-Nose in the Identification of Chinese Liquor Flavors, *IEEE Sensors Journal*, 17(6), 2017, 1788–1794.
[106] Liu, H., Li, Q., Yan, B., Zhang, L., Gu, Y., Bionic Electronic Nose Based on Mos Sensors Array and Machine Learning Algorithms Used for Wine Properties Detection, *Sensors (Switzerland)*, 19(1), 2019, 45.
[107] Wakhid, S., Sarno, R., Sabilla, S. I., Maghfira, D. B., Detection and Classification of Indonesian Civet and Non-Civet Coffee Based on Statistical Analysis Comparison Using E-Nose, *International Journal of Intelligent Engineering and Systems*, 13(4), 2020, 56–65.
[108] Xue, B., Zhang, M., Browne, W. N., Yao, X., A Survey on Evolutionary Computation Approaches to Feature Selection, *IEEE Transactions on Evolutionary Computation*, 20(4), 2016, 606–626.
[109] Khalid, S., Khalil, T., Nasreen, S., A Survey of Feature Selection and Feature Extraction Techniques in Machine Learning, *Proceedings of 2014 Science and Information Conference, SAI 2014*, 372–378, 2014.
[110] Postma, E., Van, H. J., Herik, D., van der Maaten, L. J. P., Postma, E. O., van den Herik, H. J., Dimensionality Reduction: A Comparative Review, *Journal of Machine Learning Research*, 10(1), 2008, 1-35.
[111] Hira, Z. M., Gillies, D. F., A Review of Feature Selection and Feature Extraction Methods Applied on Microarray Data, *Advances in Bioinformatics*, 2015, 2015, 198363.
[112] Pashami, S., Lilienthal, A. J., Schaffernicht, E., Trincavelli, M., TREFEX: Trend Estimation and Change Detection in the Response of MOX Gas Sensors, *Sensors (Switzerland)*, 13(6), 2013, 7323–7344.
[113] Zhang, S., Xie, C., Hu, M., Li, H., Bai, Z., Zeng, D., An Entire Feature Extraction Method of Metal Oxide Gas Sensors, *Sensors and Actuators, B: Chemical*, 132(1), 2008, 81–89.
[114] Faleh, R., Othman, M., Gomri, S., Aguir, K., Kachouri, A., A Transient Signal Extraction Method of WO3 Gas Sensors Array to Identify Polluant Gases, *IEEE Sensors Journal*, 16(9), 2016, 3123–3130.
[115] Carmel, L., Levy, S., Lancet, D., Harel, D., A Feature Extraction Method for Chemical Sensors in Electronic Noses, *Sensors and Actuators, B: Chemical*, 93(1–3), 67–76, 2003.
[116] Ziyatdinov, A., Fonollosa, J., Fernández, L., Gutiérrez-Gálvez, A., Marco, S., Perera, A., Data Set from Gas Sensor Array under Flow Modulation, *Data in Brief*, 3, 2015, 131–136.
[117] Effrosynidis, D., Arampatzis, A., An Evaluation of Feature Selection Methods for Environmental Data, *Ecological Informatics*, 61, 2021, 101224.
[118] Lee, L. C., Jemain, A. A., On Overview of PCA Application Strategy in Processing High Dimensionality Forensic Data, *Microchemical Journal*, 169, 2021, 106608.
[119] Li, G., Hu, Y., An Enhanced PCA-Based Chiller Sensor Fault Detection Method Using Ensemble Empirical Mode Decomposition Based Denoising, *Energy and Buildings*, 183, 2019, 311–324.
[120] Wang, Y., Wu, D., Yuan, X., LDA-Based Deep Transfer Learning for Fault Diagnosis in Industrial Chemical Processes, *Computers and Chemical Engineering*, 140, 2020, 106964.
[121] Leng, Y. *et al.*, LDA-Based Data Augmentation Algorithm for Acoustic Scene Classification, *Knowledge-Based Systems*, 195, 2020, 105600.
[122] Dimigen, O., Optimizing the ICA-Based Removal of Ocular EEG Artifacts from Free Viewing Experiments, *NeuroImage*, 207, 2020, 116117.
[123] Khan, M. A. H., Thomson, B., Debnath, R., Motayed, A., Rao, M. v., Nanowire-Based Sensor Array for Detection of Cross-Sensitive Gases Using PCA and Machine Learning Algorithms, *IEEE Sensors Journal*, 20(11), 2020, 6020–6028.
[124] Brems, M., A One-Stop Shop for Principal Component Analysis, *Towards Data Science*, 2017. https://towardsdatascience.com/a-one-stop-shop-for-principal-component-analysis-5582fb7e0a9c (accessed Dec. 03, 2022).
[125] Delgado, D. B., Understanding Principal Component Analysis Once And For All, *blukiri*, 2018. https://medium.com/bluekiri/understanding-principal-component-analysis-once-and-for-all-9f75e7b33635 (accessed Dec. 03, 2022).
[126] López, M. M. *et al.*, SVM-Based CAD System for Early Detection of the Alzheimer's Disease Using Kernel PCA and LDA, *Neuroscience Letters*, 464(3), 2009, 233–238.
[127] Aliyari Ghassabeh, Y., Rudzicz, F., Moghaddam, H. A., Fast Incremental LDA Feature Extraction, *Pattern Recognition*, 48(6), 2015, 1999–2012.
[128] Raschka, S., Linear Discriminant Analysis – Bit by Bit, *Sebastian Raschka*, 2014. https://sebastianraschka.com/Articles/2014_python_lda.html (accessed Dec. 03, 2022).
[129] Pinto, L. S. *et al.*, Compression Method of Power Quality Disturbances Based on Independent Component Analysis and Fast Fourier Transform, *Electric Power Systems Research*, 187, 2020, 106428.
[130] Sun, L., Liu, Y., Beadle, P. J., Independent Component Analysis of EEG Signals, *Proceedings of the 2005 IEEE International Workshop on VLSI Design and Video Technology, IWVDVT 2005*, 293–296, 2005.
[131] Huang, S. H., Supervised Feature Selection: A Tutorial, *Artificial Intelligence Research*, 4(2), 2015, 22-37.
[132] Cai, J., Luo, J., Wang, S., Yang, S., Feature Selection in Machine Learning: A New Perspective, *Neurocomputing*, 300, 2018, 70–79.
[133] Smialowski, P., Frishman, D., Kramer, S., Pitfalls of Supervised Feature Selection, *Bioinformatics*, 26(3), 2009, 440–443.
[134] Song, L., Smola, A., Gretton, A., Borgwardt, K. M., Bedo, J., Supervised Feature Selection via Dependence Estimation, *Proceedings of the 24th international conference on Machine learning - ICML '07*, 823–830, 2007.
[135] Inoue, J., Yamagata, Y., Chen, Y., Poskitt, C. M., Sun, J., Anomaly Detection for a Water Treatment System Using Unsupervised Machine Learning, *IEEE International Conference on Data Mining Workshops, ICDMW*, 2017-November, 1058–1065, 2017.
[136] Wang, S., Tang, J., Liu, H., Embedded Unsupervised Feature Selection, *AAAI'15: Proceedings of the Twenty-Ninth AAAI Conference on Artificial Intelligence*, 470–476, 2015.
[137] Sheikhpour, R., Sarram, M. A., Gharaghani, S., Chahooki, M. A. Z., A Survey on Semi-Supervised Feature Selection Methods, *Pattern Recognition*, 64, 2017, 141–158.
[138] Ang, J. C., Mirzal, A., Haron, H., Hamed, H. N. A., Supervised, Unsupervised, and Semi-Supervised Feature Selection: A Review on Gene Selection, *IEEE/ACM Transactions on Computational Biology and Bioinformatics*, 13(5), 2016, 971–989.
[139] Tang, J., Alelyani, S., Liu, H., Feature Selection for Classification: A Review, in *Data Classification: Algorithms and Applications*, 2014, 37–64.
[140] Kashef, S., Nezamabadi-pour, H., Nikpour, B., Multilabel Feature Selection: A Comprehensive Review and Guiding Experiments, *Wiley Interdisciplinary Reviews: Data Mining and Knowledge Discovery*, 8(2), 2018, e1240.
[141] Odhiambo Omuya, E., Onyango Okeyo, G., Waema Kimwele, M., Feature Selection for Classification Using Principal Component Analysis and Information Gain, *Expert Systems with Applications*, 174, 2021, 114765.
[142] Deng, C. *et al.*, Enhancing the Discrimination Ability of a Gas Sensor Array Based on a Novel Feature Selection and Fusion Framework, *Sensors (Switzerland)*, 18(6), 2018, 1909.
[143] Han, J. S., Lee, S. W., Bien, Z., Feature Subset Selection Using Separability Index Matrix, *Information Sciences*, 223, 2013, 102–118.
[144] Saeys, Y., Inza, I., Larrañaga, P., A Review of Feature Selection Techniques in Bioinformatics, *Bioinformatics*, 23(19), 2007, 2507–2517.
[145] Guo, G., Wang, H., Bell, D., Bi, Y., Greer, K., KNN Model-Based Approach in Classification, *Lecture Notes in Computer Science (including subseries Lecture Notes in Artificial Intelligence and Lecture Notes in Bioinformatics)*, 2888, 2003, 986–996.
[146] Begum, S., Chakraborty, D., Sarkar, R., Data Classification Using Feature Selection and KNN Machine Learning Approach, *Proceedings - 2015 International Conference on Computational Intelligence and Communication Networks, CICN 2015*, 811–814, 2016.
[147] Chauhan, V. K., Dahiya, K., Sharma, A., Problem Formulations and Solvers in Linear SVM: A Review, *Artificial Intelligence Review*, 52(2), 2019, 803–855.
[148] Marjanovic, M., Kovacevic, M., Bajat, B., Voženílek, V., Landslide Susceptibility Assessment Using SVM Machine Learning Algorithm, *Engineering Geology*, 123(3), 2011, 225–234.
[149] Maxwell, A. E., Warner, T. A., Fang, F., Implementation of Machine-Learning Classification in Remote Sensing: An Applied Review, *International Journal of Remote Sensing*, 39(9), 2018, 2784–2817.

[150] Sá, J. A. S., Almeida, A. C., Rocha, B. R. P., Mota, M. A. S., Souza, J. R. S., Dentel, L. M., Lightning Forecast Using Data Mining Techniques On Hourly Evolution Of The Convective Available Potential Energy, *Congresso Brasileiro de Inteligência Computacional*, Fortaleza, Ceará Brazil, 1–5, 2016.

[151] Thorson, J., Collier-Oxandale, A., Hannigan, M., Using a Low-Cost Sensor Array and Machine Learning Techniques to Detect Complex Pollutant Mixtures and Identify Likely Sources, *Sensors (Switzerland)*, 19(17), 2019, 3723.

[152] Tan, J., Xu, J., Applications of Electronic Nose (e-Nose) and Electronic Tongue (e-Tongue) in Food Quality-Related Properties Determination: A Review, *Artificial Intelligence in Agriculture*, 4, 2020, 104–115.

[153] Rubesam, A., Machine Learning Portfolios with Equal Risk Contributions: evidence from the Brazilian market, *SSRN Electronic Journal*, 2019, 1-55.

[154] Voyant, C. *et al*., Machine Learning Methods for Solar Radiation Forecasting: A Review, *Renewable Energy*, 105, 2017, 569–582.

[155] Al-Hadidi, M. R., Alarabeyyat, A., Alhanahnah, M., Breast Cancer Detection Using K-Nearest Neighbor Machine Learning Algorithm, *Proceedings - 2016 9th International Conference on Developments in eSystems Engineering, DeSE 2016*, 35–39, 2017.

[156] Polikar, R., Ensemble Based Systems in Decision Making, *IEEE Circuits and Systems Magazine*, 6(3), 2006, 21–44.

[157] Cordón, O., Kazienko, P., Trawi□ski, B., Special Issue on Hybrid and Ensemble Methods in Machine Learning, *New Generation Computing*, 29(3), 2011, 241–244.

[158] Ardabili, S., Mosavi, A., Varkonyi-Koczy, A. R., Advances in Machine Learning Modeling Reviewing Hybrid and Ensemble Methods, *In: Várkonyi-Kóczy, A. (eds) Engineering for Sustainable Future. INTER-ACADEMIA 2019. Lecture Notes in Networks and Systems*, Springer, Cham, 2020.

[159] González, S., García, S., del Ser, J., Rokach, L., Herrera, F., A Practical Tutorial on Bagging and Boosting Based Ensembles for Machine Learning: Algorithms, Software Tools, Performance Study, Practical Perspectives and Opportunities, *Information Fusion*, 64, 2020, 205–237.

[160] Abadi, M., Isard, M., Murray, D. G., A Computational Model for TensorFlow an Introduction, *MAPL 2017 - Proceedings of the 1st ACM SIGPLAN International Workshop on Machine Learning and Programming Languages, co-located with PLDI 2017*, 1–7, 2017.

[161] Karamchandani, S., Sekhani, B., Nair, K., Shah, K., E-Nose for Shelf-Life Prediction of Climacteric Fruits, *2021 IEEE 4th International Conference on Computing, Power and Communication Technologies, GUCON 2021*, 2021.

[162] Wei, H., Gu, Y., A Machine Learning Method for the Detection of Brown Core in the Chinese Pear Variety Huangguan Using a Mos-Based e-Nose, *Sensors (Switzerland)*, 20(16), 2020, 1–15.

[163] Liu, H., Yu, D., Gu, Y., Classification and Evaluation of Quality Grades of Organic Green Teas Using an Electronic Nose Based on Machine Learning Algorithms, *IEEE Access*, 7, 2019, 172965–172973.

[164] Wang, Q., Qi, H., Liu, F., Time Series Prediction of E-Nose Sensor Drift Based on Deep Recurrent Neural Network, *2019 Chinese Control Conference (CCC)*, 3479–3484, 2019.

[165] Mo, Z., Luo, D., Wen, T., Cheng, Y., Li, X., FPGA Implementation for Odor Identification with Depthwise Separable Convolutional Neural Network, *Sensors (Switzerland)*, 21(3), 2021, 1–19.

[166] Paszke, A. *et al*., Automatic Differentiation in PyTorch, *31st Conference on Neural Information Processing Systems (NIPS)*, 2017.

[167] Pedregosa, F. *et al*., Scikit-Learn: Machine Learning in Python, *Journal of Machine Learning Research*, 12, 2012, 2825–2830.

[168] Banerjee, M. B., Roy, R. B., Tudu, B., Bandyopadhyay, R., Bhattacharyya, N., Black Tea Classification Employing Feature Fusion of E-Nose and E-Tongue Responses, *Journal of Food Engineering*, 244, 2019, 55–63.

[169] Gharpure, D., Kukade, M., Moshayedi, A. J., Kukade, M. V., Gharpure, D. C., Electronic-Nose (E-Nose) for Recognition of Cardamom, Nutmeg and Clove Oil Odor, *Electronics and its Interdisciplinary Applications* (NC AE IA - 2014) at: Fergusson College, Pune, Maharashtra, 2014.

[170] Galang, M. G. K., Zarra, T., Naddeo, V., Belgiorno, V., Ballesteros, F., Artificial Neural Network in the Measurement of Environmental Odours by E-Nose, *Chemical Engineering Transactions*, 68, 2018, 247–252.

[171] Hall, M., Frank, E., Holmes, G., Pfahringer, B., Reutemann, P., Witten, I. H., The WEKA Data Mining Software, *ACM SIGKDD Explorations Newsletter*, 11(1), 2009, 10–18.

[172] Han, J., Rodriguze, J. C., Beheshti, M., Diabetes Data Analysis and Prediction Model Discovery Using RapidMiner, *Proceedings of the 2008 2nd International Conference on Future Generation Communication and Networking, FGCN 2008 and BSBT 2008: 2008 International Conference on Bio-Science and Bio-Technology*, 3, 96–99, 2008.

[173] Dietz, C., Berthold, M. R., KNIME for Open-Source BioImage Analysis-A Tutorial, *In: De Vos, W., Munck, S., Timmermans, JP. (eds) Focus on Bio-Image Informatics. Advances in Anatomy, Embryology and Cell Biology*, Springer, 2016.

[174] Sonnenburg, S. *et al*., The SHOGUN Machine Learning Toolbox, *Journal of Machine Learning Research*, 11, 2010, 1799–1802.

[175] Adnan, K. N. A. K. *et al*., Water Quality Classification and Monitoring Using E-Nose and e-Tongue in Aquaculture Farming, *2014 2nd International Conference on Electronic Design, ICED 2014*, 343–346, 2014.

[176] Jasinski, G., Wozniak, L., Kalinowski, P., Jasinski, P., Evaluation of the Electronic Nose Used for Monitoring Environmental Pollution, *2018 15th International Scientific Conference on Optoelectronic and Electronic Sensors, COE 2018*, 2018.

[177] Jha, S. K., Hayashi, K., A Novel Odor Filtering and Sensing System Combined with Regression Analysis for Chemical Vapor Quantification, *Sensors and Actuators, B: Chemical*, 200, 2014, 269–287.

[178] Rodríguez-Aguilar, M. *et al*., Identification of Breath-Prints for the COPD Detection Associated with Smoking and Household Air Pollution by Electronic Nose, *Respiratory Medicine*, 163, 2020, 105901.

[179] Conti, P. P., Andre, R. S., Mercante, L. A., Fugikawa-Santos, L., Correa, D. S., Discriminative Detection of Volatile Organic Compounds Using an Electronic Nose Based on TiO2 Hybrid Nanostructures, *Sensors and Actuators, B: Chemical*, 344, 2021, 130124.

[180] Wang, Q. *et al*., Discrimination of Mutton from Different Sources (Regions, Feeding Patterns and Species) by Mineral Elements in Inner Mongolia, China, *Meat Science*, 174, 2021, 108415.

[181] Mahmodi, K., Mostafaei, M., Mirzaee-Ghaleh, E., Detection and Classification of Diesel-Biodiesel Blends by LDA, QDA and SVM Approaches Using an Electronic Nose, *Fuel*, 258, 2019, 116114.

[182] Özsandikcio□lu, Ü., Atasoy, A., Yapici, □., Hybrid Sensor Based E-Nose for Lung Cancer Diagnosis, *MeMeA 2018 - 2018 IEEE International Symposium on Medical Measurements and Applications, Proceedings*, 2018.

[183] Liu, B. *et al*., Lung Cancer Detection via Breath by Electronic Nose Enhanced with a Sparse Group Feature Selection Approach, *Sensors and Actuators, B: Chemical*, 339, 2021, 129896.

[184] Mohamed, E. I., Khalil, G. I., Abdel-Mageed, S. M., Bayoumi, A. M., Ramadan, H. S., Kotb, M. A., Electronic Noses for Monitoring Benzene Occupational Exposure in Biological Samples of Egyptian Workers, *International Journal of Occupational Medicine and Environmental Health*, 26(1), 2013, 165–172.

[185] Durán Acevedo, C. M., Carrillo Gómez, J. K., Albarracín Rojas, C. A., Academic Stress Detection on University Students during COVID-19 Outbreak by Using an Electronic Nose and the Galvanic Skin Response, *Biomedical Signal Processing and Control*, 68, 2021, 102756.

[186] Dragonieri, S. *et al*., An Electronic Nose in the Discrimination of Patients with Asthma and Controls, *Journal of Allergy and Clinical Immunology*, 120(4), 2007, 856–862.

[187] Marom, O., Nakhoul, F., Tisch, U., Shiban, A., Abassi, Z., Haick, H., Gold Nanoparticle Sensors for Detecting Chronic Kidney Disease and Disease Progression, *Nanomedicine*, 7(5), 2012, 639–650.

[188] Ezhilan, M., Nesakumar, N., Babu, K. J., Srinandan, C. S., Rayappan, J. B. B., Freshness Assessment of Broccoli Using Electronic Nose, *Measurement: Journal of the International Measurement Confederation*, 145, 2019, 735–743.

[189] Sanaeifar, A., Li, X., He, Y., Huang, Z., Zhan, Z., A Data Fusion Approach on Confocal Raman Microspectroscopy and Electronic Nose for Quantitative Evaluation of Pesticide Residue in Tea, *Biosystems Engineering*, 210, 2021, 206–222.

[190] Ghasemi-Varnamkhasti, M., Mohammad-Razdari, A., Yoosefian, S. H., Izadi, Z., Siadat, M., Aging Discrimination of French Cheese Types Based on the Optimization of an Electronic Nose Using Multivariate Computational Approaches Combined with Response Surface Method (RSM), *LWT*, 111, 2019, 85–98.

[191] Li, P., Niu, Z., Shao, K., Wu, Z., Quantitative Analysis of Fish Meal Freshness Using an Electronic Nose Combined with Chemometric Methods, *Measurement: Journal of the International Measurement Confederation*, 179, 2021, 109484.

[192] Yin, X., Zhang, L., Tian, F., Zhang, D., Temperature Modulated Gas Sensing E-Nose System for Low-Cost and Fast Detection, *IEEE Sensors Journal*, 16(2), 2016, 464–474.

[193] Salhi, L., Silverston, T., Yamazaki, T., Miyoshi, T., Early Detection System for Gas Leakage and Fire in Smart Home Using Machine Learning, *2019 IEEE International Conference on Consumer Electronics (ICCE)*, 1–6, 2019.

[194] Binson, V. A., Subramoniam, M., Design and Development of an E-Nose System for the Diagnosis of Pulmonary Diseases, *Acta of Bioengineering and Biomechanics*, 23(1), 2021, 35-44.

[195] le Maout, P. *et al.*, Polyaniline Nanocomposites Based Sensor Array for Breath Ammonia Analysis. Portable e-Nose Approach to Non-Invasive Diagnosis of Chronic Kidney Disease, *Sensors and Actuators, B: Chemical*, 274, 2018, 616–626.

[196] Gardner, J. W., Shin, H. W., Hines, E. L., Dow, C. S., An Electronic Nose System for Monitoring the Quality of Potable Water, *Sensors and Actuators B: Chemical*, 69(3), 2000, 336–341.

[197] Capone, S., Epifani, M., Quaranta, F., Siciliano, P., Taurino, A., Vasanelli, L., Monitoring of Rancidity of Milk by Means of an Electronic Nose and a Dynamic PCA Analysis, *Sensors and Actuators B: Chemical*, 78(1–3), 2001, 174-179.

[198] Zhang, H., Wang, J., Ye, S., Chang, M., Application of Electronic Nose and Statistical Analysis to Predict Quality Indices of Peach, *Food and Bioprocess Technology*, 5(1), 2012, 65–72.

[199] Baskar, C., Nesakumar, N., Balaguru Rayappan, J. B., Doraipandian, M., A Framework for Analysing E-Nose Data Based on Fuzzy Set Multiple Linear Regression: Paddy Quality Assessment, *Sensors and Actuators, A: Physical*, 267, 2017, 200–209.

[200] Javed, U. *et al.*, Quantification of Gas Concentrations in NO/NO2/C3H8/NH3 Mixtures Using Machine Learning, *Sensors and Actuators B: Chemical*, 359, 2022, 131589.

[201] Javed, U., Ramaiyan, K. P., Kreller, C. R., Brosha, E. L., Mukundan, R., Morozov, A. V., Using Sensor Arrays to Decode NOx/NH3/C3H8 Gas Mixtures for Automotive Exhaust Monitoring, *Sensors and Actuators, B: Chemical*, 264, 2018, 110–118.

[202] Tsitron, J. *et al.*, Bayesian Decoding of the Ammonia Response of a Zirconia-Based Mixed-Potential Sensor in the Presence of Hydrocarbon Interference, *Sensors and Actuators, B: Chemical*, 192, 2014, 283–293.

[203] Wilson, A. D., Review of Electronic-Nose Technologies and Algorithms to Detect Hazardous Chemicals in the Environment, *Procedia Technology*, 1, 2012, 453–463.

[204] Sironi, S., Eusebio, L., Capelli, L., Remondini, M., del Rosso, R., Use of an Electronic Nose for Indoor Air Quality Monitoring, *Chemical Engineering Transactions*, 40(Special Issue), 2014, 73–78.

[205] Moufid, M., Bouchikhi, B., Tiebe, C., Bartholmai, M., el Bari, N., Assessment of Outdoor Odor Emissions from Polluted Sites Using Simultaneous Thermal Desorption-Gas Chromatography-Mass Spectrometry (TD-GC-MS), Electronic Nose in Conjunction with Advanced Multivariate Statistical Approaches, *Atmospheric Environment*, 256, 2021, 118449.

[206] Tsakanikas, P., Karnavas, A., Panagou, E. Z., Nychas, G. J., A Machine Learning Workflow for Raw Food Spectroscopic Classification in a Future Industry, *Scientific Reports*, 10(1), 2020, 11212.

[207] Lei, J. *et al.*, Detection of Ammonia Based on a Novel Fluorescent Artificial Nose and Pattern Recognition, *Atmospheric Pollution Research*, 7(3), 2016, 431–437.

[208] Pyatt, F. B., Potential Effects on Human Health of an Ammonia Rich Atmospheric Environment in an Archaeologically Important Cave in Southeast Asia, *Occupational and Environmental Medicine*, 60(12), 2003, 986–988.

[209] Liao, Y. H., Hsiao, Y. J., Nagarjuna, Y., Shieh, J. S., The Micro-Electro-Mechanical Systems (MEMS) Gas Sensor with Bilayer SnO2/WO3 Films for Ammonia Detection, *Microsystem Technologies*, 28, 2022, 287–293.

[210] Guo, L. *et al.*, Design and Fabrication of Micro-Nano Fusion Gas Sensor Based on Two-Beam Micro-Hotplatform, *Microsystem Technologies*, 23(7), 2017, 2699–2705.

[211] Prajesh, R., Jain, N., Agarwal, A., Low Power Highly Sensitive Platform for Gas Sensing Application, *Microsystem Technologies*, 22(9), 2016, 2185–2192.

[212] Kumar, R., Kumar, P., Kumar, Y., Time Series Data Prediction Using IoT and Machine Learning Technique, *Procedia Computer Science*, 167, 2020, 373–381.

[213] Pace, C., Khalaf, W., Latino, M., Donato, N., Neri, G., E-Nose Development for Safety Monitoring Applications in Refinery Environment, *Procedia Engineering*, 47, 2012, 1267–1270.

[214] Nath, S., Dey, A., Pachal, P., Sing, J. K., Sarkar, S. K., Performance Analysis of Gas Sensing Device and Corresponding IoT Framework in Mines, *Microsystem Technologies*, 27(11), 2021, 3977–3985.

[215] Rea, H., McAuley, S., Stewart, A., Lamont, C., Roseman, P., Didsbury, P., A Chronic Disease Management Programme Can Reduce Days in Hospital for Patients with Chronic Obstructive Pulmonary Disease, *Internal Medicine Journal*, 34(11), 2004, 608–614.

[216] Menke, A., Orchard, T. J., Imperatore, G., Bullard, K. M. K., Mayer-Davis, E., Cowie, C. C., The Prevalence of Type 1 Diabetes in the United States, *Epidemiology*, 24(5), 2013, 773–774.

[217] Hegde, P. S., Chen, D. S., Top 10 Challenges in Cancer Immunotherapy, *Immunity*, 52(1), 2020, 17–35.

[218] Brinkman, P. *et al.*, Exhaled Volatile Organic Compounds as Markers for Medication Use in Asthma, *European Respiratory Journal*, 55(2), 2020, 1900544.

[219] Chang, J. E. *et al.*, Analysis of Volatile Organic Compounds in Exhaled Breath for Lung Cancer Diagnosis Using a Sensor System, *Sensors and Actuators, B: Chemical*, 255, 2018, 800–807.

[220] Vajhadin, F., Mazloum-Ardakani, M., Amini, A., Metal Oxide-Based Gas Sensors for the Detection of Exhaled Breath Markers, *Medical Devices & Sensors*, 4(1), 2020, e10161.

[221] Li, W., Jia, Z., Xie, D., Chen, K., Cui, J., Liu, H., Recognizing Lung Cancer Using a Homemade E-Nose: A Comprehensive Study, *Computers in Biology and Medicine*, 120, 2020, 103706.

[222] Chen, K. *et al.*, Recognizing Lung Cancer and Stages Using a Self-Developed Electronic Nose System, *Computers in Biology and Medicine*, 131, 2021, 104294.

[223] Nawaz, M. S., Shoaib, B., Ashraf, M. A., Intelligent Cardiovascular Disease Prediction Empowered with Gradient Descent Optimization, *Heliyon*, 7(5), 2021, e06948.

[224] Tozlu, B. H., ⊠im⊠ek, C., Aydemir, O., Karavelioglu, Y., A High Performance Electronic Nose System for the Recognition of Myocardial Infarction and Coronary Artery Diseases, *Biomedical Signal Processing and Control*, 64, 2021, 102247.

[225] Hong, J. *et al.*, Retinopathy and Risk of Kidney Disease in Persons with Diabetes, *Kidney Medicine*, 3(5), 2021, 808–815.

[226] Voss, A. *et al.*, Smelling Renal Dysfunction via Electronic Nose, *Annals of Biomedical Engineering*, 33(5), 2005, 656–660.

[227] Saidi, T., Zaim, O., Moufid, M., el Bari, N., Ionescu, R., Bouchikhi, B., Exhaled Breath Analysis Using Electronic Nose and Gas Chromatography–Mass Spectrometry for Non-Invasive Diagnosis of Chronic Kidney Disease, Diabetes Mellitus and Healthy Subjects, *Sensors and Actuators, B: Chemical*, 257, 2018, 178–188.

[228] Benedek, P., Lázár, Z., Bikov, A., Kunos, L., Katona, G., Horváth, I., Exhaled Biomarker Pattern Is Altered in Children with Obstructive Sleep Apnoea Syndrome, *International Journal of Pediatric Otorhinolaryngology*, 77(8), 2013, 1244–1247.

[229] Liao, Y. H., Shih, C. H., Abbod, M. F., Shieh, J. S., Hsiao, Y. J., Development of an E-Nose System Using Machine Learning Methods to Predict Ventilator-Associated Pneumonia, *Microsystem Technologies*, 28, 2022, 341–351.

[230] Kanaparthi, S., Singh, S. G., Discrimination of Gases with a Single Chemiresistive Multi-Gas Sensor Using Temperature Sweeping and Machine Learning, *Sensors and Actuators B: Chemical*, 348, 2021, 130725.

[231] Mohd Ali, M., Hashim, N., Abd Aziz, S., Lasekan, O., Principles and Recent Advances in Electronic Nose for Quality Inspection of Agricultural and Food Products, *Trends in Food Science and Technology*, 99, 2020, 1–10.

[232] Wojnowski, W., Majchrzak, T., Dymerski, T., G⊠bicki, J., Namie⊠nik, J., Portable Electronic Nose Based on Electrochemical Sensors for Food Quality Assessment, *Sensors (Switzerland)*, 17(12), 2017, 2715.

[233] Kodogiannis, V. S., Application of an Electronic Nose Coupled with Fuzzy-Wavelet Network for the Detection of Meat Spoilage, *Food and Bioprocess Technology*, 10(4), 2017, 730–749.

[234] Papadopoulou, O. S., Panagou, E. Z., Mohareb, F. R., Nychas, G. J. E., Sensory and Microbiological Quality Assessment of Beef Fillets Using a Portable Electronic Nose in Tandem with Support Vector Machine Analysis, *Food Research International*, 50(1), 2013, 241–249.

[235] Wijaya, D. R., Sarno, R., Zulaika, E., DWTLSTM for Electronic Nose Signal Processing in Beef Quality Monitoring, *Sensors and Actuators, B: Chemical*, 326, 2021, 128931.

[236] Qiu, S., Wang, J., The Prediction of Food Additives in the Fruit Juice Based on Electronic Nose with Chemometrics, *Food Chemistry*, 230, 2017, 208–214.

[237] Srivastava, S., Mishra, G., Mishra, H. N., Fuzzy Controller Based E-Nose Classification of Sitophilus Oryzae Infestation in Stored Rice Grain,

Food Chemistry, 283, 2019, 604–610.
[238] Tanaka, F., Magariyama, Y., Miyanoshita, A., Volatile Biomarkers for Early-Stage Detection of Insect-Infested Brown Rice: Isopentenols and Polysulfides, *Food Chemistry*, 303, 2020, 125381.
[239] Kumari, L., Jaiswal, P., Tripathy, S. S., Various Techniques Useful for Determination of Adulterants in Valuable Saffron: A Review, *Trends in Food Science and Technology*, 111, 2021, 301–321.
[240] Mobasseri, M. *et al.*, Effects of Saffron Supplementation on Glycemia and Inflammation in Patients with Type 2 Diabetes Mellitus: A Randomized Double-Blind, Placebo-Controlled Clinical Trial Study, *Diabetes & Metabolic Syndrome: Clinical Research & Reviews*, 14(4), 2020, 527–534.
[241] Kiani, S., Minaei, S., Ghasemi-Varnamkhasti, M., Integration of Computer Vision and Electronic Nose as Non-Destructive Systems for Saffron Adulteration Detection, *Computers and Electronics in Agriculture*, 141, 2017, 46–53.
[242] Kiani, S., Minaei, S., Ghasemi-Varnamkhasti, M., A Portable Electronic Nose as an Expert System for Aroma-Based Classification of Saffron, *Chemometrics and Intelligent Laboratory Systems*, 156, 2016, 148–156.
[243] Gradišek, A. *et al.*, Improving the Chemical Selectivity of an Electronic Nose to TNT, DNT and RDX Using Machine Learning, *Sensors (Switzerland)*, 19(23), 2019, 5207.
[244] Wang, Y., Xing, J., Qian, S., Selectivity Enhancement in Electronic Nose Based on an Optimized DQN, *Sensors (Switzerland)*, 17(10), 2017, 2356.
[245] Zhang, L., Liu, Y., He, Z., Liu, J., Deng, P., Zhou, X., Anti-Drift in E-Nose: A Subspace Projection Approach with Drift Reduction, *Sensors and Actuators, B: Chemical*, 253, 2017, 407–417.
[246] Rehman, A. U., Bermak, A., Drift-Insensitive Features for Learning Artificial Olfaction in E-Nose System, *IEEE Sensors Journal*, 18(17), 2018, 7173–7182.
[247] Latha, R. S., Lakshmi, P. K., Electronic Tongue: An Analytical Gustatory Tool, *Journal of Advanced Pharmaceutical Technology and Research*, 3(1), 2012, 3–8.
[248] Apetrei, I. M., Apetrei, C., Voltammetric E-Tongue for the Quantification of Total Polyphenol Content in Olive Oils, *Food Research International*, 54(2), 2013, 2075–2082.
[249] Rodríguez-Méndez, M. L. *et al.*, Electronic Noses and Tongues in Wine Industry, *Frontiers in Bioengineering and Biotechnology*, 4, 2016, 81.
[250] Buratti, S., Malegori, C., Benedetti, S., Oliveri, P., Giovanelli, G., E-Nose, e-Tongue and e-Eye for Edible Olive Oil Characterization and Shelf Life Assessment: A Powerful Data Fusion Approach, *Talanta*, 182, 2018, 131–141.

ORCID iD

Lubna Mahmood https://orcid.org/0000-0002-8142-992X
Mehdi Ghommem https://orcid.org/0000-0002-8451-8805
Zied Bahroun https://orcid.org/0000-0003-2832-3672

How to cite this article: Mahmood L., Ghommem M., Bahroun Z. Smart Gas Sensors: Materials, Technologies, Practical Applications, and Use of Machine Learning – A Review, *J. Appl. Comput. Mech.*, 9(3), 2023, 775–803. https://doi.org/10.22055/jacm.2023.41985.3851